University of Southern Queensland

Faculty of Health, Engineering and Sciences

Implementation of Automated LVDT Calibration for Fatigue and Fracture Laboratory

A dissertation submitted by

Aaron Mietzel

In fulfillment of the requirements of

ENG4111 and ENG4112 Research Project

towards the degree of

Bachelor of Engineering (Honours) (Mechatronic)

Submitted October, 2023

Abstract

Calibration is an important process for allowing the comparison of values from a tested measuring device against another device of known measuring accuracy. The process is inextricable in ensuring metrological integrity by establishing and maintaining traceability of measuring equipment and its higher standard references. Possessing an accuracy reference provides confidence to the user of such equipment that the value of measure being obtained is reliable. For this reason, many industries are dependent on their measuring devices to undergo periodic calibration, which in large quantities, can result in delays to commence work activities. One such case where a testing environment has experienced such delays is within the Defence Science and Technology Group's Fatigue and Fracture Laboratory. Linear Displacement Transducers are used in a large number of the laboratory's test programmes and are calibrated on-site using an outdated calibration process that is time consuming and requires constant operator manual input throughout the entire process.

This report explores the potential improvements to calibration time and operator manual effort by introducing an automated variation of the Fatigue and Fracture Laboratory's calibration process.

A review of current literature was conducted to understand the following: the working concept of displacement transducers; detailed steps involved in the old system calibration process; calibration requirements for linear displacement transducers as per the National Association of Testing Authorities' Scope of Accreditation.

The methodology details the design and construction of the new automated linear displacement calibration system, which comprises two main sections: the displacer subsystem; the voltmeter subsystem. An explanation is also provided on the steps taken to measure the new automated subsystems against their old subsystem counterparts as an accuracy reference. This was done as the old subsystems were accepted under the Scope of Accreditation.

With a functioning system, a testing regime was conducted to measure the total calibration time and time of operator manual input. This was performed using both systems where the results between the systems were compared. Two groups participated in the trials: one group of two operators experienced in the use of the old system; one group of two operators not experienced with the old system. By obtaining results from the two groups, it could be ascertained whether the outcomes of the new system might be consistent across operator experience levels.

The results from the calibration trials yielded the following key information:

1. Significant improvements were achieved in total calibration time when using the new automated system.
2. A reduction in the operator manual input time was achieved when using the new system due to the automated process.
3. Calibration time was less dependent on operator experience when using the new system, with significantly less variation in results between all operators compared to the old system.
4. The new automated system allowed calibration to be performed by users with little or no understanding of linear displacement calibration and still conduct the process faster than an experienced operator using the old system.

The additional implication this work has on the calibration Scope of Accreditation has been evaluated and the required adjustment to the measuring capability in the accreditation has been noted in the report.

University of Southern Queensland

Faculty of Health, Engineering and Sciences

ENG4111 and 4112 Research Project

Limitations of Use

Certification

I certify that the ideas, designs, experimental work, results, analyses and conclusions set out in this dissertation are entirely my own effort, except where otherwise indicated and acknowledged.

I further certify that the work is original and has not been previously submitted for assessment in any other course or institution, except where specifically stated.

Aaron S. Mietzel
Student Number: [redacted]

Acknowledgements

I would like to thank my work supervisor Matthew Pelosi for his review, encouragement, and engaging thought over the years. My thanks also go to my colleagues who participated in my research experiments.

I give thanks to my university supervisors Tobias Low and Craig Lobsey, for the time they provided during my studies.

Lastly, I would like to thank my partner Nadezhda, who has supported my ideas, ambitions and shared with me all that is dear with the greatest gift of all.

Table of Contents

List of Figures

List of Tables

Abbreviations

AC	Alternating current
ADC	Analogue-to-digital Converter
DC	Direct current
DSTG	Defence Science & Technology Group
EMI	Electromagnetic Interference
EMF	Electromotive force
FFL	Fatigue and Fracture Laboratory
FSR	Full-scale range
IDE	Interactive Development Environment
IEC	International Electrotechnical Commission
ISO	International Organization for Standardization
LDT	Linear Displacement Transducer
LVDT	Linear Variable Displacement Transducer
MS-DOS	Microsoft Disk Operating System
NATA	National Association of Testing Authorities
PGA	Programmable gain amplifier
SMTC	Structures and Materials Test Centre

1. Introduction

1.1. Background and Problem Identification

This research project seeks to evaluate the feasibility of a bespoke improvement to an established Linear Variable Differential Transformer (LVDT) calibration method used within a testing environment at a Defence Science & Technology Group (DSTG) research facility. DSTG is a Department of Defence agency that provides scientific and technological solutions to safeguard Australia and its national interests (DSTG 2023). A component of the agency's responsibilities involves efforts towards capability enhancement and asset sustainment for the Department of Defence. Within the DSTG Aerospace Platform Systems group, sustainment operations are supported by the Structures and Materials Test Centre (SMTC), a state-of-the-art facility in materials and structural testing that specialises in fatigue testing of aircraft structures (DSTG 2023). Facilitating the SMTC in fatigue testing and research is the Fatigue and Fracture Laboratory (FFL), which does this by performing a variety of small-scale material and component testing under various loading conditions, such as static and spectrum-based dynamic loading applications. It is important for the outcome of such procedures that the resulting test data is producible with high integrity. This demands the utilisation of the appropriate measuring equipment with accurate signal acquisition and processing. It is therefore, that metrology exists as an inherently crucial consideration within the FFL, where its activities consequently rely significantly on the appropriate calibration of laboratory testing equipment. To ensure the FFL retains accreditation with current internationally accepted testing and calibration processes, the laboratory undergoes a regular auditing process performed by the National Association of Testing Authorities (NATA) (an Australian accreditation body for international laboratory standards) for evaluation of laboratory compliance with the international standard ISO/IEC 17025, i.e., 'General requirements for the competence of testing and calibration laboratories' (Standards Australia 2018). Hence, data produced within the accredited laboratory is done so with recognised and traceable standardised practices, ensuring acceptable performance and calibration of all measuring equipment used in the process. Such equipment comprises load cells, extensometers, LVDTs and other displacement transducers – all of which must remain within calibration when in service.

1.2. LVDT Calibration and Laboratory Testing

LVDTs are used in various applications where the measurement of linear displacement is required. As such, LVDTs are found in many systems supporting industry activities such as automation, hydraulic power, manufacturing, aerospace platform control and many others. Common functions in a laboratory setting include, for example, axial piston control or valve position control.

So too are these LVDT functions important in DSTGs testing laboratories where LVDTS are used alongside actuators for measuring the displacement of testing coupons, articles and platform components under load. An example of an FFL system that utilises an LVDT can be seen in Figure 1. The image depicts a typical hydraulic servo-valve testing machine equipped with an LVDT to measure the displacement of the piston rod. A test coupon is mounted in the upper and lower grips where the upper grip is made stationary by a locked crosshead while the load (and consequent resulting displacement) is applied through the lower grip mounted to the piston rod. Assuming no slippage of the test article occurs within the grips, the LVDT measure is indicative of the displacement applied.

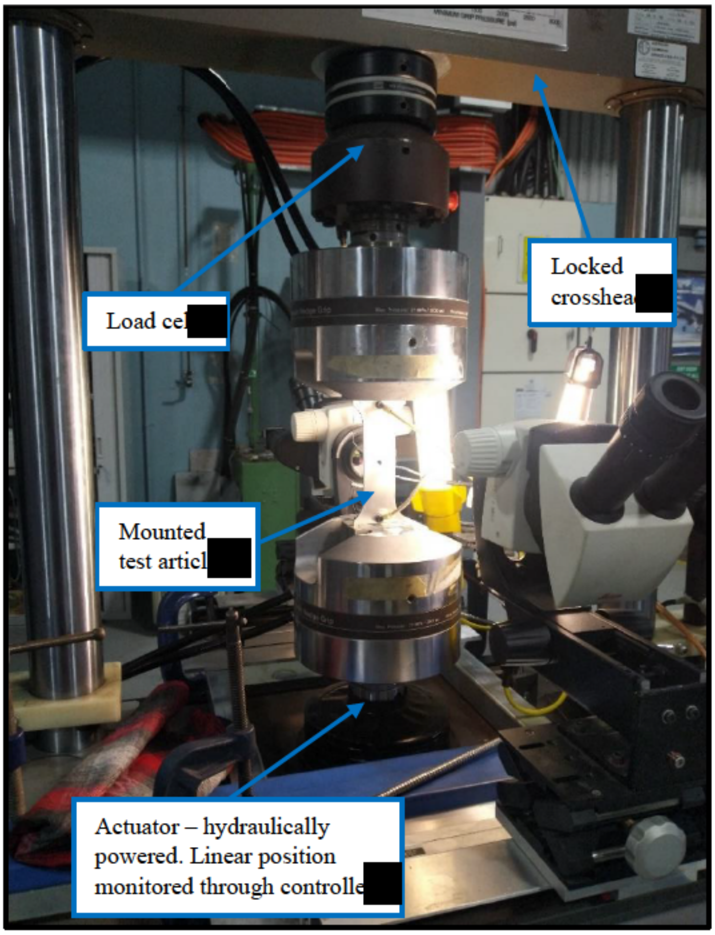

Figure 1 – Image of an MTS 100 kN servo-hydraulic testing frame used in the FFL. A coupon is mounted for axial loading through the lower grip-equipped actuator.

It is important for the fore-mentioned applications that the integrity of the LVDT linear displacement measurements is ensured. For example, in the test application illustrated in Figure 1, one of the methods of control is displacement which utilizes the measurements from an LVDT in the actuator as the source for feedback control (MTS 2009, p. 33). As such, some testing procedures are designed specifically around physical displacement of the testing article, (e.g., ramp rate of 'x' mm per minute to failure). As a safety response, in either displacement or load control, all testing procedures have a variety of 'limits' in place that cease hydraulic power to the actuator when exceeded. This includes a displacement limit of the axial range. If the LVDT is not appropriately calibrated, it cannot be understood to what degree the signal being read from the LVDT is truly representative of the physical displacement of the actuator.

Considering the examples provided respectively, in the event of an inaccurate or faulty LVDT, the situation could result in an incorrect measure of displacement in ramp rate testing, or, undershooting/overshooting of axial displacement due to inappropriate setting of axial displacement limits (the latter of which might also impose crushing or over-tensioning in the test article). To ensure the performance of an LVDT, the unit undergoes calibration. Calibration involves a process of measurement that assigns values to a response of an instrument relative to a reference standard or to a "designated reference process" (NIST 2012). The difference between the reference sensor voltage and the output of the sensor being calibrated is defined as the 'calibration factor' (MTS 2009, p. 44). The calibration procedure is usually a scheduled one for units in service. Therefore, given many LVDTs are in service within the SMTC, there is an ongoing need to perform calibration.

1.3. Problem Identification

A problem has been identified in instances where an SMTC activity, in support of a test programme or platform-usage investigation, may require access to a large number of LVDTs in a short time frame, thereby requiring a large number of calibrations to be completed within a deadline. The FFL, being responsible for the activity, relies on an outdated system to perform the calibration. While the current system provides the tools necessary for calibration as is accepted under the NATA accreditation, the process itself while using this system is a time-restrictive one, requiring lab-personnel manual operation that is susceptible to human error (see Section 2.2 for the process description).

1.4. Aim

The goal of this research project is to design and construct a system with the capability to automatically perform and process LVDT calibration measurements. The system is to offer improvements over the current DSTG FFL calibration procedure, namely: a reduction in the total time of operation (i.e., time taken for displacement and subsequent signal measurement); and the minimum manual input required by laboratory staff to perform the operation and record the data. Given that the system is to support an FFL activity, the potential benefits and disadvantages within the context of laboratory work requirements, will be appropriately evaluated against the same parameters for the current system. Furthermore, given the FFL NATA accreditation to the international standard ISO/IEC 17025 (see Appendix E for NATA Scope of Accreditation), it will be observed whether FFL compliance with the standard can be maintained with the implementation of the proposed automated system.

1.5. Objectives

To ensure the necessary actions are taken to address the aim of this research task, it is necessary to assign a set of objectives that are deemed suitable as a guideline and as milestones to completion. The research objectives are as follows:

1.5.1. Background Research

Access to background information and literature relevant to this work is necessary to understand what knowledge is available and which contributions have been performed in this area. This includes details of the following: the function of an LVDT; design and application of other automated LVDT calibration systems; the specific LVDT models calibrated by the FFL; components and operation of the currently used LVDT calibration system (including current work instruction guideline) and; the scope of the FFL's NATA accreditation.

1.5.2. Prototype Hardware Design

It is necessary that the proposed automated system be designed with respect to a set of specifications where the function of the resulting system would satisfy the calibration task. This will involve the evaluation and subsequent selection of available components.

1.5.3. Development of Code

Once the requirements are satisfied for the physical system, an appropriate code is required to operate the system. This objective in the project is what enables the automatic control to take place and therefore, will require the design with consideration in mind of minimum operator input and automatic acquisition and processing of LVDT-measured values.

1.5.4. System Trials

The automated LVDT calibrator prototype will be used in a trial that compares the time taken to perform and process calibration measurements compared to that of the old procedure. The second element of the trials will be to evaluate the amount of time operator manual input is required (including manual height gauge displacement and recording of data). The sample size will comprise two groups: personnel trained in the operation of the old system and; personnel not trained in its operation.

1.5.5. Feasibility Analysis

In addition to an analysis of the results from the proposed trials outlined in Section 1.5.4 to observe potential operational benefits of an automated system, it is also necessary to determine whether the new system provides enough accuracy such that the calibration results fall within the scope of NATA Accreditation. Depending on this outcome and if time permits, adjustments may be made to satisfy this requirement.

1.6. Consequences and Ethics

The current process for LVDT calibration within DSTG is dependent on an aging system that is demanding on operator input time to complete. Should the outcome of this research project result in a successful system implementation, the proposed system would replace the need for operator manual input with an automated calibration procedure. This would comprise relief both in terms of user manual displacement of the LVDT via a height gauge and, the recording of measurements saved into a text document. The implications are an improvement to calibration time and a reduction in human error by eliminating the need for human input where possible. Moreover, since all components used to develop the system are low-cost and easy to access, the laboratory can consider opting for a replacement maintenance strategy when servicing the system components rather than be dependent on a system that can amount to numerous months of down time due to required maintenance by skilled service personnel. The proposed system, however, will require a basic understanding of how to operate it from a command window and how to physically configure the external devices i.e., the LVDT to the controller, power supply to the LVDT, mounting the LVDT as well as external power supply to the controller.

Ethical considerations to be made are minimal in this work. The most notable element is that of integrity of data. All measurements taken should be defined with a level of measurement uncertainty. This should be documented to provide metrological performance and calibration traceability. The work conducted in this research task will evaluate this point considerably with an observation made regarding the effect of introduced measurement uncertainty on the FFL's scope of NATA accreditation (see Appendix E).

2. Literature Review

2.1. LVDTs

Transducers are defined as devices that have the capability to convert a signal from one source to an electrical signal, and vice versa. An example of this can be observed in generators, where the application of mechanical energy to a shaft converts the energy to electrical. The reverse is true, where conversely, an electrical signal that is applied to the coil in a generator, will produce mechanical motion, hence, acting as a motor. Examples of transducers are numerous, demonstrating the conversion to electrical energy from many natural phenomena such as, light (light-dependent resistors), sound (microphones), temperature (thermistors), and force (load cells) just to name a few. The ability to convert these signals to an electrical one provides a convenient way to measure and process information about the natural environment. In addition to the aforementioned applications, transducers play an important role in the measurement of physical distances. The linear displacement of an object can be measured using a Linear Variable Differential Transformer (LVDT) (or, Linear Variable Displacement Transducer interchangeably), which is an electromechanical position transducer. The device consists of primary and secondary windings with a magnetic component, such as a rod or ring and, depending on the type of LVDT, can be powered by either alternating current (AC) or direct current (DC) signal. An example of a typical AC-powered LVDT can be seen in Figure 2 below:

Figure 2 – an LVDT consisting of primary and secondary windings and a linearly displaceable magnetic core rod (Lord Sensing 2022).

AC-powered LVDTs comprise a primary coil of current carrying conductor windings, and a two symmetrically placed secondary coils placed in series with an identical number of windings to each other. The device functions by providing an excitation voltage through the primary coil, which, in the presence of a magnetic field provided by a ferrite core, induces an alternating current within the secondary coils. Hence, the transducer is also defined as a 'transformer', as the induction obeys Faraday's Law, which states: "The voltage induced across a coil of wire equals the number of turns in the coil times the rate of change of the magnetic flux" (Floyd 2009, p. 393).

$$V_{ind} = N\left(\frac{d\Phi}{dt}\right)$$

Where:

v_{ind} is the induced voltage
N is the number of windings in a coil of a current carrying conductor
Φ is the magnetic flux

The series-connected secondary coils of the LVDT are wired such that the electromotive force (EMF) induced in them oppose each other (see Figure 3). Therefore, when the magnetic core is equally distanced from the two secondary windings (i.e., in the middle position), the induced EMF produced in both are of equal magnitude but opposite in direction ($180°$ out of phase), thus producing a “null” output (Alciatore & Histand 2012, p. 380).

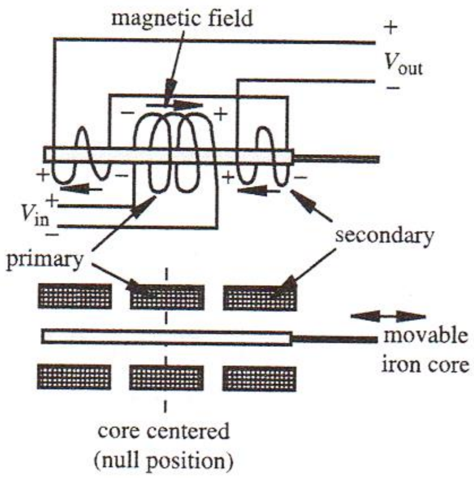

Figure 3 - Diagram of AC LVDT winding configuration relative to the moveable magnetic core (Alciatore & Histand 2012, p. 381)

By applying an AC signal to the primary coil, an induced AC signal in the secondary coil is produced. When the magnetic core is displaced from the zero position, a change in the magnetic field within the coils occurs. The greater the displacement, the lesser is the amount of core in one of the secondary windings and therefore, the greater the EMF difference between the two secondary windings. Therefore, by monitoring the change in the net output voltage (or secondary winding voltage difference), the amount of magnetic core displacement can be observed (Bolton 1999, p. 27). The direction and magnitude of magnetic core change is linearly proportional to the amplitude of the voltage output, (see Figure 4).

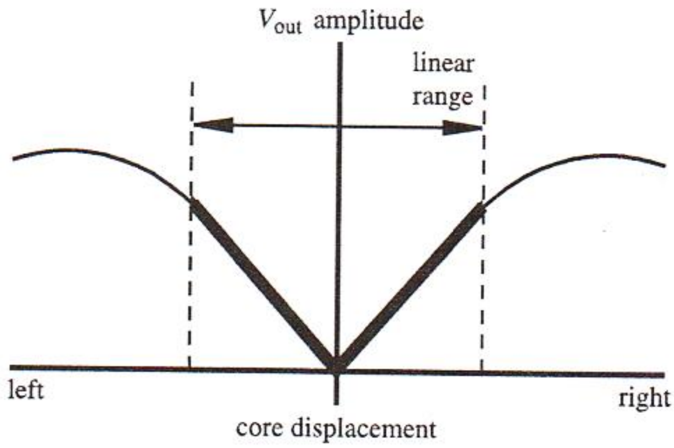

Figure 4 – The linear relationship window between magnetic core displacement and the output voltage amplitude (Alciatore & Histand 2012, p. 381).

This design relies on mutual inductance, as can been seen in the equation for determining the secondary coil induced EMF ‘e’ due to a primary coil change in current ‘i’, (Bolton 1999, p. 27):

$$e = M\frac{di}{dt}$$

Where:

e is the EMF
i is the current
M is the mutual inductance, as below (Libretexts Physics 2022).

$$M = \frac{N_2\Phi_1}{i_1}$$

Where:

N_2 is the number of turns of the secondary coil
Φ_1 is magnetic field produced by the current in the primary coil
i_1 is the current in the primary coil.

The usual operating range of an LVDT is approximately between ±2 mm to ±400 mm with non-linearity errors of roughly $\pm0.25\%$ (Bolton 1999, p. 28).

Advantages of the LVDT are that it provides good accuracy within its linear range, is less susceptible to external influences over other displacement transducers, such as the effects of temperature (Bolton 1999, p. 28) and provides excellent repeatability with frictionless measurements. Disadvantages of the AC LVDT include: susceptibility to electromagnetic interference (thus potentially necessitating shielding); the dependence on a circuit modulator to rectify the AC signal and produce a DC signal; and a low-pass filter to smooth the rectified signal (see Figure 5), which restricts the frequency response range of the LVDT.

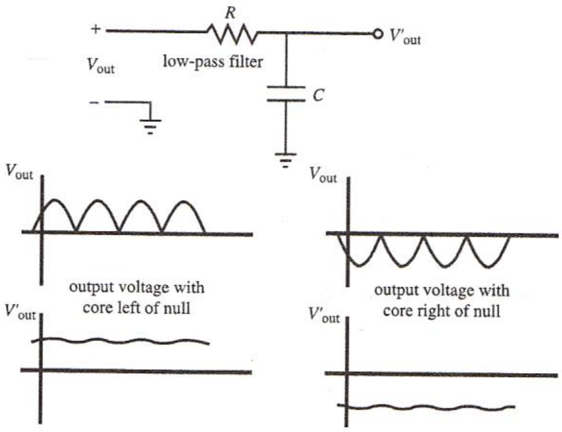

Figure 5 – A low-pass filter circuit and the effect it produces on the LVDT output signal (Alciatore & Histand 2012, p. 382).

With developments in electronics technology, the manufacture of integrated circuits has become possible. For transducers, this means that any additional electronics that would normally be required external to a transducer, could now be integrated densely within the unit. This technology is utilised to produce DC-DC type LVDTs incorporating the working principles of the standard AC LVDT. This is done by integrating into the AC LVDT, the necessary signal conditioning electronics to convert a DC input signal to AC, followed by demodulation at the output. Figure 6 illustrates a block diagram of this process.

1. The provided DC input passes through reverse polarity protection and voltage regulation
2. An oscillator is used to convert the signal from DC to AC
3. The signal is processed as per the working principles of an AC LVDT
4. The differential output proceeds to a demodulator integrated circuit that rectifies the circuit back to DC and passes through a low-pass filter to smooth the circuit.
5. Finally, amplification of the DC output occurs.

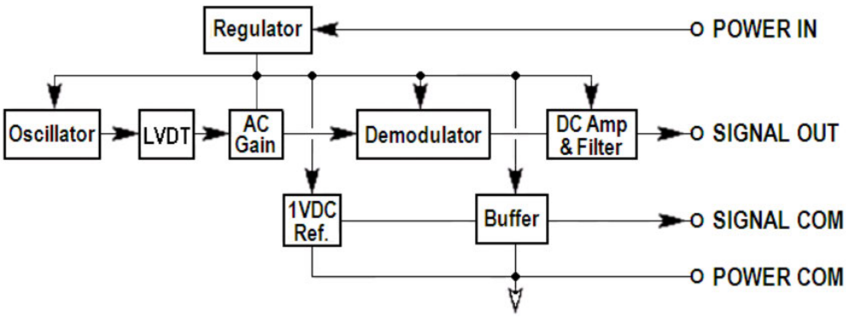

Figure 6 - Block diagram of general-purpose DC LVDT signal conditioning process (TE Connectivity 2017)

The advantage of using a DC LVDT is that linear displacement measurement is possible with the use of DC signals, while still retaining the benefits of LVDT frictionless displacement and accurate linearity.

2.1.1. Temposonics Linear Position Sensor

The FFL is equipped with numerous in-service Temposonics linear position sensors that work with contactless measurement utilising an externally adjustable magnet (see Figure 7).

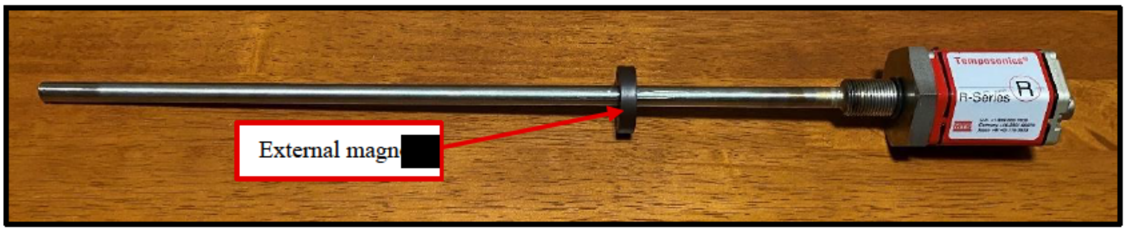

Figure 7 - Tempsonics R-Series Model RH rod-style position sensor with single magnet

These devices work using an MTS-developed magnetostriction sensing principle which consists of high-accuracy measuring of the time taken for a sonic pulse to travel to the external magnet and back to the sensing element. The return pulse is produced through the interaction of two magnetic fields (Temposonics 2022). One of which being that produced by the adjustable external magnetic, and the other generated by the 'interrogation pulse' which is applied through the waveguide to interact with the external magnet magnetic field. A magnetostriction working principle illustration can be seen in Figure 8.

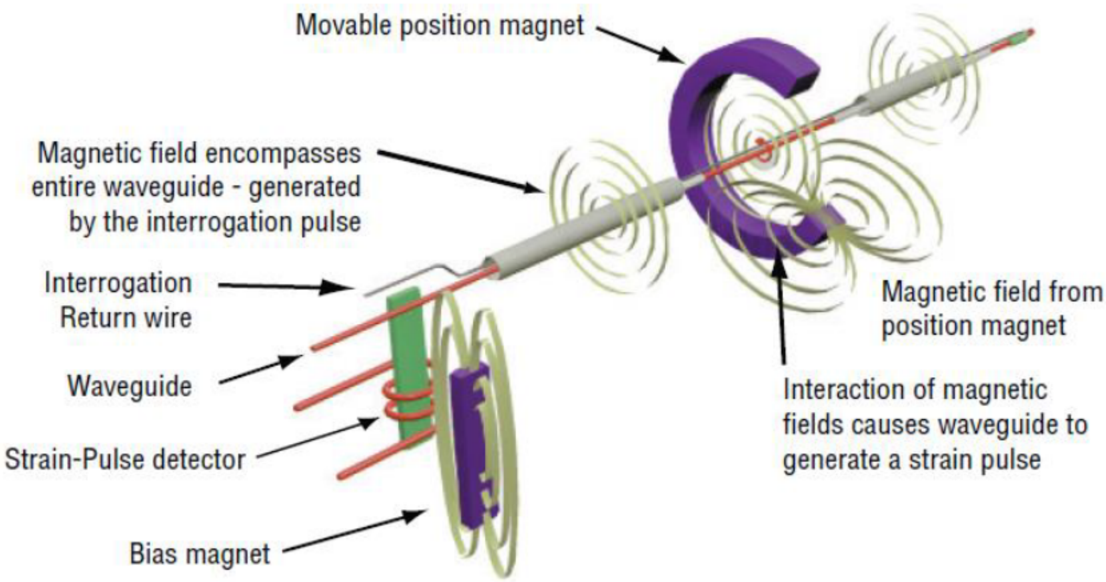

Figure 8 – Time-based Magnetostrictive position sensing working principle (Temposonics 2022, p. 1)

The Temposonics linear position sensor can be operated either externally in application for linear displacement measurement, or as an internal installation such as in fluid cylinders (e.g., hydraulic lines). For the internal configuration, the sensor head can remain external for access (see Figure 9).

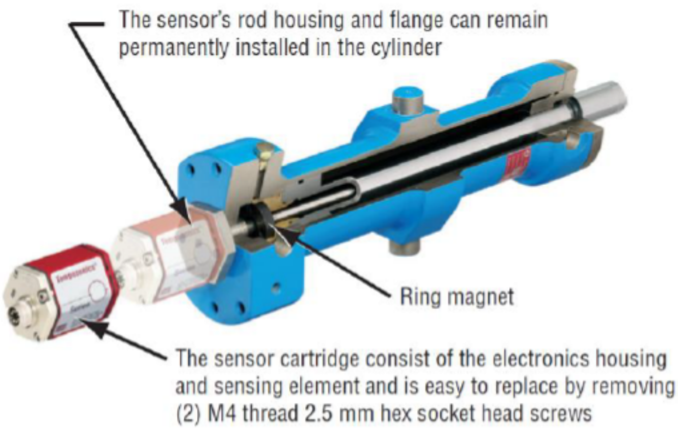

Figure 9 – An internally configured Temposonics R-Series Model RH for a fluid cylinder (Temposonics 2022, p. 9)

2.2. Current System

The following components make up the devices used in the current system (referred to in Chapters 3 and onwards as the 'old system') to perform the calibration of displacement transducers.

2.2.1. HP 3458A Multimeter

The calibrated voltmeter used in the current system and shown in Figure 10, is the 8.5-digit HP 3458A. Equipped with front and rear 2- and 4-wire inputs with offset compensation, 10 nV sensitivity, 100,000 samples per second and 0.1 ppm DCV transfer accuracy (Agilent 2000).

Figure 10 – Image of the HP 3458A Multimeter that is used for voltage measurement in the current FFL LVDT calibration system.

2.2.2. Height Gauge

Figure 11 depicts the Trimos Model TVM602 height gauge with a 1 metre displacement range. The height gauge is equipped with a position locking mechanism, a mounting point and a dial for vertical displacement. The device is the calibrated standard used in the current calibration procedure for producing the linear displacement of the LVDT magnetic core (see Figure 2) or Linear Displacement Transducer (LDT) external magnet (see Figure 7) with a resolution of 1μm.

Figure 11 – Image of Trimos height gauge. Used in the calibration of linear position transducers to perform vertical displacement.

2.3. Fatigue and Fracture Laboratory Calibration and Work Instruction

The current system for LVDT and LDT calibration uses both the HP 3458A voltmeter (see Section 2.2.1) and the Trimos vertical height gauge (see Section 2.2.2) as part of the data acquisition system and linear displacement method respectively. Both devices function as the reference standard when performing calibration to within laboratory accreditation. The operation of the system is guided by a work instruction titled 'Calibration of Displacement Transducers' (DSTG 2019). The periodically audited document serves as both an aid in training of the current laboratory calibration procedure as well as an ongoing reference. The work instruction outlines the distinction between the displacement transducer types present in the laboratory and how to calibrate them. These include: the single primary/dual secondary winding LVDTs equipped with an adjustable and frictionless magnetic core (see Figure 2) and; the LDT design that operates on the measurement of time between an output pulse and return pulse across an operating range affected by a linearly adjustable external magnet (see Figure 7). The mounting requirements of the various displacement transducers are similar and, are usually done so manually using either a clamping method, or with the aid of a slotted bracket that results in sensor rod alignment perpendicular to the ground (or flat surface). Important is that either sensing device is positioned such that its magnetic component's displacement occurs parallel to the height gauge column, as seen in Figure 12. The image also illustrates the mounted arm used as the contact point between the Trimos height gauge and the Temposonics R-series external magnet. By performing the displacement therefore, the magnetic position is also physically adjusted and, so too does the output signal.

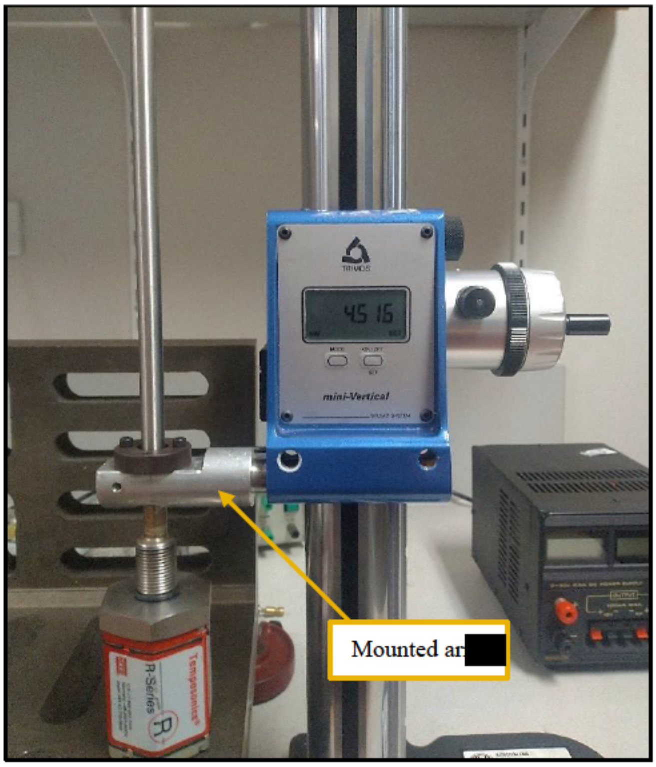

Figure 12 – Image demonstrating the mounting position of the Temposonics linear position sensor relative to the Trimos height gauge. The magnet is fixed to the arm's flat section and remains contactless with the rod upon position adjustment.

The Trimos height gauge column measures 1 metre long. It is therefore capable of applying the displacement over the entire range of all position transducers present in the FFL and hence, across their full signal ranges (either 0 to 10V or -10 to +10V). The output wires of the sensor are connected to the HP 3458A voltmeter through which the live signal is measured and displayed as shown in Figure 10.

2.3.1. Current Calibration and Data Recording Process

Following the LDT/LVDT position mounting, wiring configuration and startup of the data capture system seen in Figure 13, calibration using the current procedure begins by adjusting and 'zeroing' the height gauge at the position where the magnet of the transducer produces an output of 0V. The dial of the height gauge is rotated to displace the magnet to a minimum of 20% of the sensor linear range. After which, the dial position is locked and a sample of the output is taken and displayed on the data acquisition system monitor (Figure 14), then recorded by hand in a table. The steps are repeated for the remaining 20% intervals over the entire sensor range and repeated in reverse to arrive back at the 0V (or 0mm) position (resulting in 10 recordings). This is treated as one 'run' and is repeated for a total of 3 runs. The outcome provides a minimum of 30 readings that are then manually recorded into an Excel spreadsheet to be processed into a calibration report. The entire process is performed for each device requiring calibration, which can amount to extended times to complete.

Figure 13 – Current data capture user interface. The ‘GO’ menu is selected to begin sampling of the measured signal as seen in Figure 10.

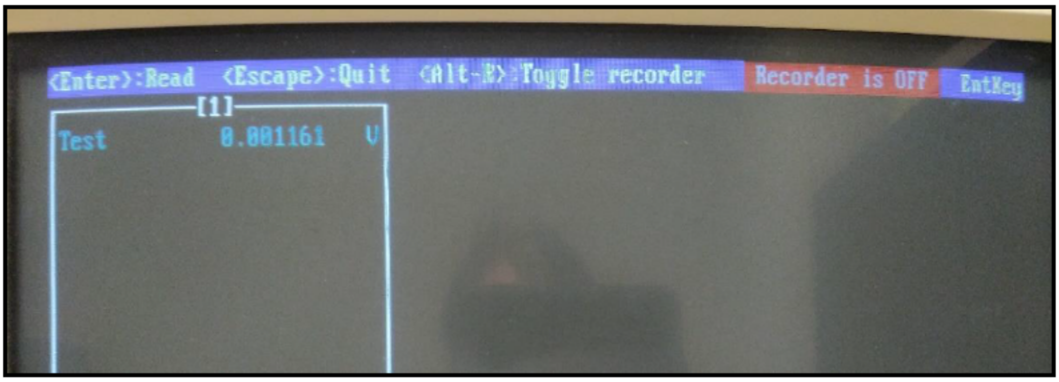

Figure 14 – The current system data capture screen displaying the value sampled from the measured LVDT signal.

The HP Data Acquisition System uses the outdated Microsoft Disk Operating System (MS-DOS) 6.22 for user control. The only present technology in the system for data transfer is a floppy drive, with which modern computers are no longer equipped. Coupled with the DSTG organisation network security policy, it is for this reason that the current system requires additional data recording by hand to transfer to another system for processing.

Figure 15 depicts an overview of the current system setup comprising: the computer used to load MS-DOS and provide a user trigger for data sampling; the HP data acquisition input; the sensor power supply; string potentiometer and; the Trimos vertical height gauge. The HP 3458A voltmeter is obscured in the image, as annotated in Figure 15. Extensive details on the system’s operation can be found in the ‘Calibration of Displacement Transducers’ work instruction (DSTG 2019, p. 7-8).

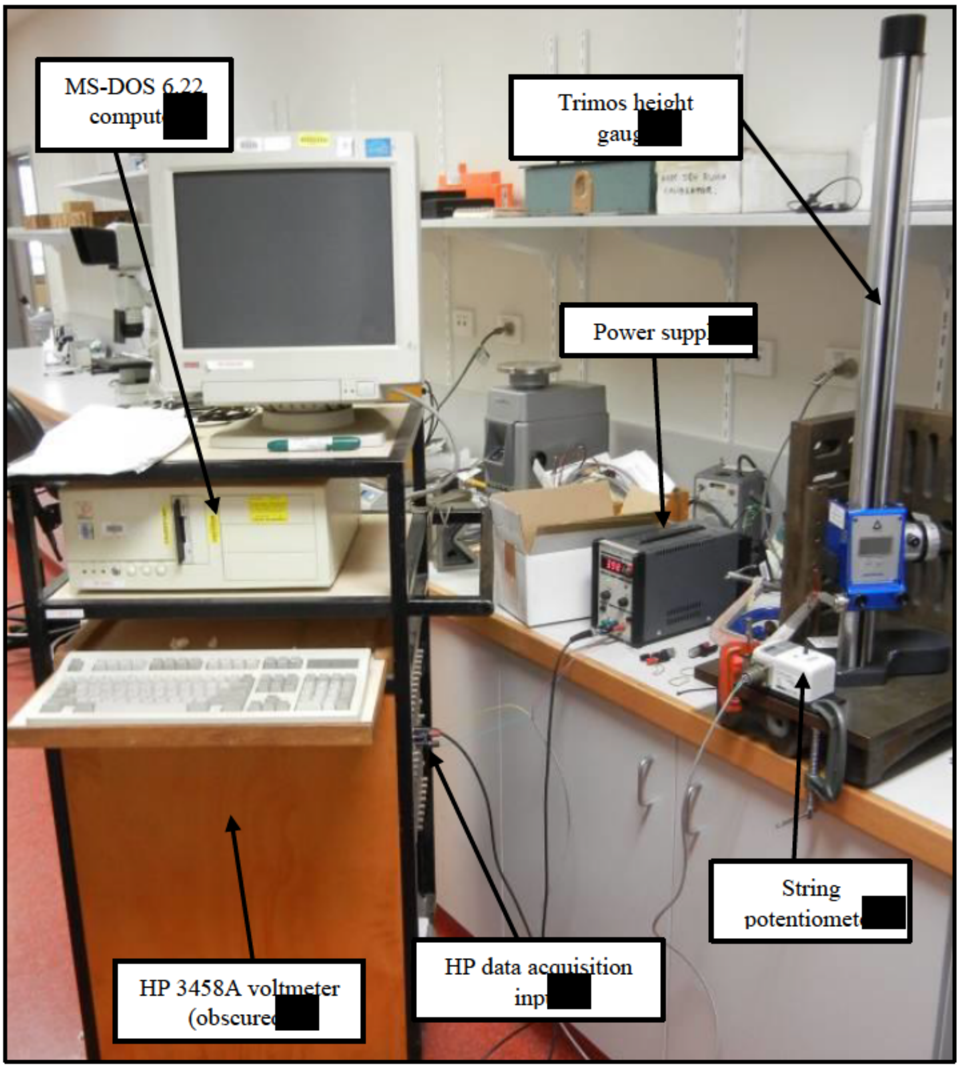

Figure 15 – Depiction of the setup used for the data acquisition displacement transducer signals (DSTG 2019, p. 18). Note, The HP3458A voltmeter is obscured in the image and its location annotated.

2.4. NATA and Testing/Calibration Accreditation – ISO/IEC 17025

The work performed within this research report is to provide novel laboratory capability to facilitate the Fatigue and Fracture Laboratory calibration of LVDTs. The FFL is NATA accredited to the international ISO/IEC 17025:2018 standard, which requires the conformance of the FFL with the standard for testing and calibration operations. NATA defines the process of accreditation as a way to "recognise, determine and promote the ability of organisations that perform specific types of technical and scientific activities" (NATA 2023). As an Australian leading national accreditation body, NATA is recognized by government to assess, award and audit accreditation to numerous standards relating to laboratory practices and proficiency testing schemes (NATA 2023), one of which being the ISO/IEC 17025, which ensures valid laboratory testing results through compliance with the standard. The ISO/IEC 17025 standard details a variety of requirements to be adhered to as well as guidelines and recommendations to consider for the holder of accreditation to achieve valid laboratory results. These include in part (Standards Australia 2018):

- General requirements of impartiality and confidentiality (Clause 4.1 and 4.2).
- Structural requirements for responsible management of operations and staff (Clause 5.1).
- Resource requirements such as personnel, environmental conditions, metrological traceability and provision of external products and services (Clause 6).
- Process requirements including in part: contracts; verification and validation; sampling/handling of test/calibration items; technical records; measurement uncertainty; validity of results and reporting (Clause 7).
- Management system requirements and guidelines (Clause 8).

Comprising the FFL NATA scope of accreditation is the proficiency to perform LVDT calibrations (see Appendix E for Scope of Accreditation). Within the scope, LVDT calibration falls under the service of “Dimensional metrology – engineering equipment and precision instruments”, with a calibration measurement capability of an accuracy of 0.0044mm over a range of 0 mm to 600 mm.

This means, that for any calibration performed on an LVDT over a 0mm to 600 mm range, the worst-case measurement uncertainty (refer to ISO/IEC 17025 Clause 7.6) results in displacement measurement of no greater than $\pm$0.0044 mm.

As per the ISO standard, the entire calibration process and acquisition of the results is to be documented for traceability, as stated under Clause 6.5.1 of the standard: “the laboratory shall establish and maintain metrological traceability of its measurement results by means of a documented unbroken chain of calibrations, each contributing to the measurement uncertainty”.

It is with this statement in mind, that for the currently accredited FFL LVDT calibration activity, any factors introduced or removed, deriving from process, equipment or operator influence shall be documented and made acknowledged its effect on the measurement uncertainty, thereby satisfying the requirements of traceability.

3. Methodology

This research project required the steps necessary to design and construct a functioning system that could successfully perform automated LVDT calibrations. In order to achieve this, the methodology was considered in line with the objectives set out in Section 1.5. Crucial to the success of this research was to possess a reasonable familiarisation with the old calibration system that was already in use in the FFL (see Section 2.3), as well as an understanding of the function of the LVDTs that are commonly used in the FFL (see Section 2.1.1). With the aforementioned knowledge, it was only then possible to begin to design and construct a new automated variation of the LVDT calibration system (see Sections 3.2 to 3.6) with the goal of operational and manual time reduction in mind. Each subsystem was designed and tested against the old system counterpart for establishing any measurement uncertainty contributed by the subsystems (refer to Sections 3.2 and 3.3). The measurement uncertainty factor was evaluated for its effect on the FFL NATA scope of accreditation for LVDT calibration (Section 4.4). With a functioning system constructed, a series of trials were performed as per Section 3.1, to verify the system performance.

3.1. Testing Regime

The following trials consisted of a two-group sample size comprising: two operators experienced in the old manual calibration process; two operators inexperienced in the old manual calibration process. The values observed in the trials were: operation 'completion time' and the 'user input time', i.e., time of operator manual effort.

a) The first calibration trials in both groups were performed using the old manual calibration system to establish a baseline of comparative results for each group. For the inexperienced group, the process was first demonstrated such that any difference between operator times would be a factor of experience and not time taken for system familiarisation.

b) The time of operation was measured from the beginning to end of the calibration operation as per the process outlined in Section 2.3.1. The entire old system process was a manual one, therefore, the 'completion time' was always equal to the 'user input time'. Each operator would perform two trials resulting in a total of 8 results (see Appendix A.1).

c) Calibration trials in both groups were performed using the new automated system. Prior to testing, a demonstration was provided for all operators on the initial manual setup and the subsequent steps to perform the automated calibration measurements (Section 3.2).

d) For each operator, the total calibration time was recorded as the 'completion time' and the initial manual setup time was recorded as the 'user input time'. Each operator would perform two trials resulting in a total of 8 results (see Appendix A.2).

e) The results were compared to determine the feasibility of utilising the automated calibration system in terms of: operation time; experience required for minimal duration of operation; manual effort required. See Section 4.2 for summary results.

3.2. Design and Construction

3.2.1. Displacer Subsystem

A major subsystem of LVDT calibration equipment was one that would provide the ability to physically displace the LVDT external magnet (Section 2.1.1). Linear displacement must also have been capable under electrical control given that the proposed system was to be automated. That is, all actuation was to be performed via a controller output. The necessary design choices were first made to construct an appropriate displacer subsystem. This was followed by calibration of the proposed subsystem relative to the displacer subsystem equivalent of the old system. By comparing this to the old subsystem, a measurement uncertainty could be determined with reference to the standard currently accepted under NATA accreditation. Sections 3.1.1 to 3.1.5 detail the design choices and construction of the displacer subsystem.

3.2.1.1. Motor and Driver

It was apparent that the most important factors for displacement within the automated LVDT calibration system, were the abilities to: displace small increments linearly; achieve repeatability; provide electrical control. These factors were realised with the selection and implementation of a stepper motor in the displacer design. This also provided the added benefit of being low-cost, in-line with the remainder of the system's components. A Nema 17 stepper motor (Figure 16) was used which provided a fixed angular displacement of 1.8° per pulse to the motor with a rated voltage and current of 3.06V and 1.7A respectively (see motor datasheet in Appendix G.1).

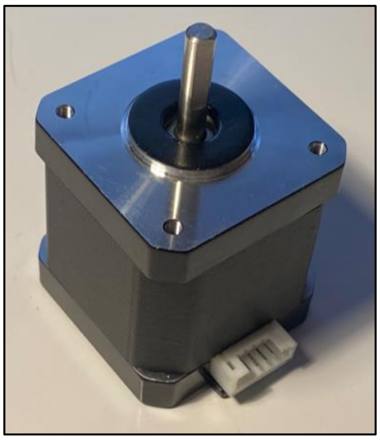

Figure 16 – Nema 17 Stepper Motor with a 'D-cut' (flat-sided) shaft.

As stated above, producing as small an angular displacement as possible per pulse was an important factor, one that may not have been fulfilled by 1.8°. Finer increments were achieved with a function of the stepper motor driver module DRV8825, selected for use in the displacer design.

The DRV8825 (Figure 17) produces a maximum of 32 intervals for a single step of a stepper motor step, i.e., applying 32 pulses (as opposed to one) to a 200-step stepper motor resulted in one step (or 1.8° rotation). The driver has a peak output current of 3A and features directional control (Texas Instruments 2014).

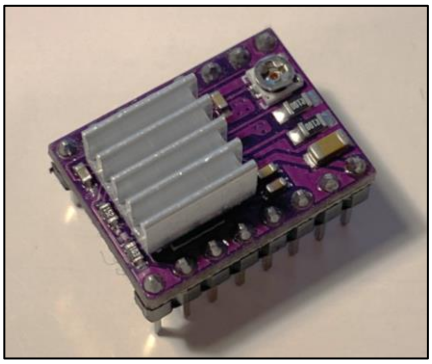

Figure 17 – DRV8825 stepper motor driver module

3.2.1.2. Ball Screw, Linear Rail and Mounting Blocks

Due to limited funding, a decision was made to utilise low-cost components for the assembly of the mechanical aspect of the linear actuator system. It was understood that in satisfying this condition, there would be a necessity to find an appropriate method for joining all the components together, as the linear rail block and the ball screw brass nut block that came standard with the low-cost components, did not have any convenient means of attachment without further machining of the blocks. Any drilling of the mounting/guide block holes was opted against as it may have presented an obstacle for the fastening of the LVDT attachment arm (Figure 23), which was to be designed in a later phase. It was decided that a 3D model would be produced with 3D CAD software and then 3D printed to determine whether a feasible fit could be created to attach the linear rail block and ball screw nut block, thus combining the linear rail (Figure 18) and ball screw system (Figure 19).

Figure 18 - SBR12 600 mm linear rail and guide block.

Figure 19 – SFU1204 550 mm ball screw, BK/BF10 bearing blocks, spindle and coupling.

Figure 20d shows the bracket designed that allowed for the successful attachment of the linear rail and ball screw components of the system. The system also comprised two bearing blocks and one stepper motor (Figure 16). It was important that these components were in-line with the ball screw as the bearings would provide the end supports and low-friction rotational capability, while the stepper motor shaft would transfer the rotational motion to the ball screw shaft, in turn displacing the mounting block across the thread and guide block along the linear rail. For this setup to be effective, it was therefore necessary that both the stepper motor shaft and bearing centrelines were colinear with the centreline of the ball screw thread (Figure 22).

3.2.1.3. 3D Models of Linear Actuator Mounting Brackets

Given that access to a 3D printer was available, it was decided that 3D models would be used to create the housing of the bearing blocks and stepper motor. The 3D designs of the housing components were done such that the appropriate height was achieved to produce collinearity among all component centrelines. Figures 20a to 20d depict the 3D models that were printed and used in the final construction.

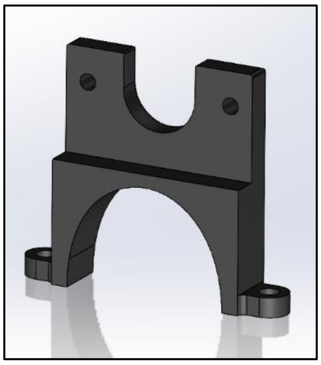

Figure 20a – Bearing block housing no.1

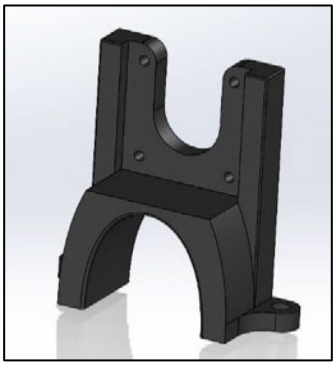

Figure 20b – Stepper motor housing

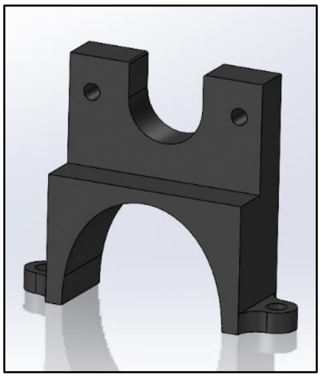

Figure 20c – Bearing block housing no.2

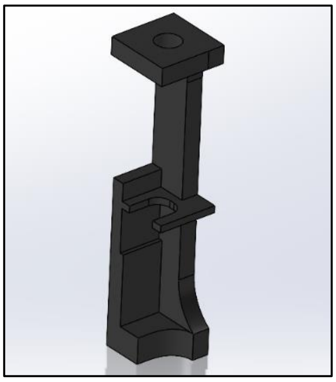

Figure 20d – Linear actuator rail and ball screw attachment bracket

The 3D assembly model illustrated in Figure 21 illustrates how the attachment bracket (Figure 20d) was used to attach the linear guide rail and ball screw components of the system by mating the mounting block and sliding block. As seen in Figure 22, the bearing block and stepper motor housing provided not only the mounting of their respective components, but through the appropriate fastening position to the system base, the correct alignment and height of all system components was achieved.

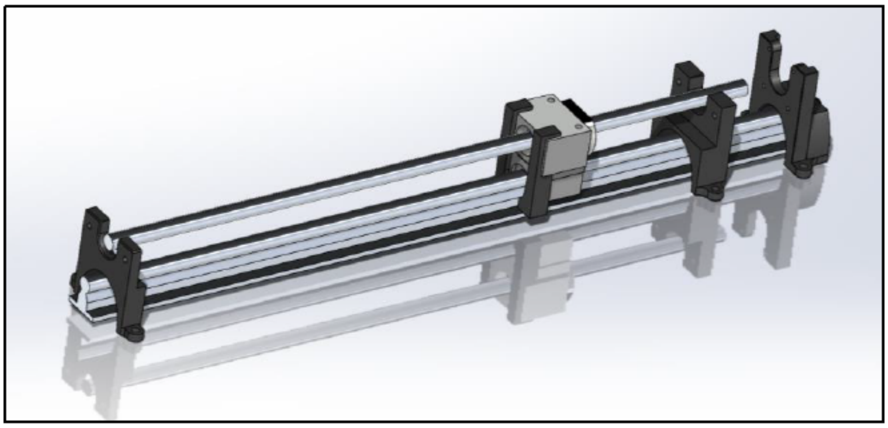

Figure 21 – 3D image of the assembly model of the linear actuator system comprising the 3D printed mounting brackets.

3.2.1.4. Constructed Linear Actuator System

Figure 22 shows the constructed linear actuator prototype with the following labelled components as indicated in the figure:

1. First bearing block and 3D-printed block housing (see Figure 21a "reference 3D model").
2. 600 mm linear rail.
3. Ball screw threaded shaft with an operating range of 400 mm.
4. Attachment point of the ball screw to the linear rail. The rail guiding block and ball screw brass nut block are mated with bespoke left and right 3d-printed attachment brackets (see Figure 20d "reference 3D model").
5. Roller limit switch and 3D-printed housing.
6. Second bearing block and 3D-printed block housing (see Figure 20c "reference 3D model").
7. Shaft coupler for joining the ball screw shaft and the stepper motor shaft.
8. Nema17 stepper motor and 3D-printed motor housing (see Figure 20b "reference 3D model").

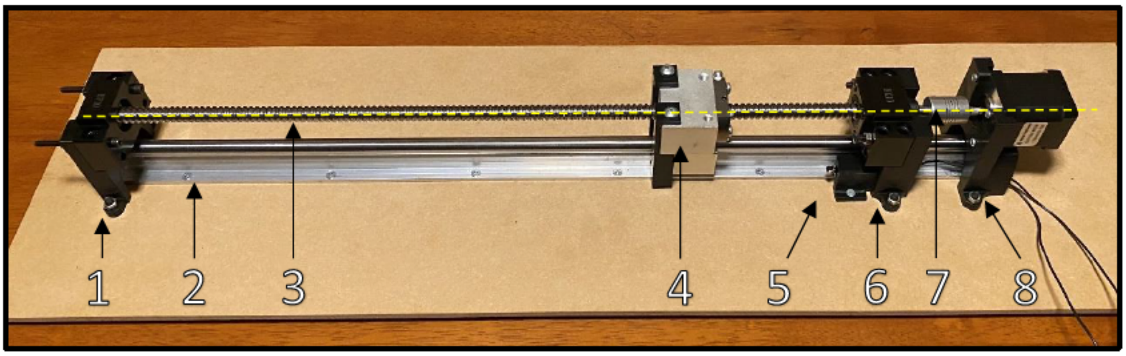

Figure 22 - Constructed linear actuator system without an LVDT mounted. The centreline is illustrated as well as the numerical annotation provided to indicate the separate components of the system detailed in Section 3.2.1.

Figure 23 shows the attachment arm that was later fastened onto the ball screw mounting block (indicated by annotation no. 4 in Figure 22) and onto which the external magnet is attached to the 'O' section. The completed setup can be seen in Figure 33 of Section 3.2.3.4.

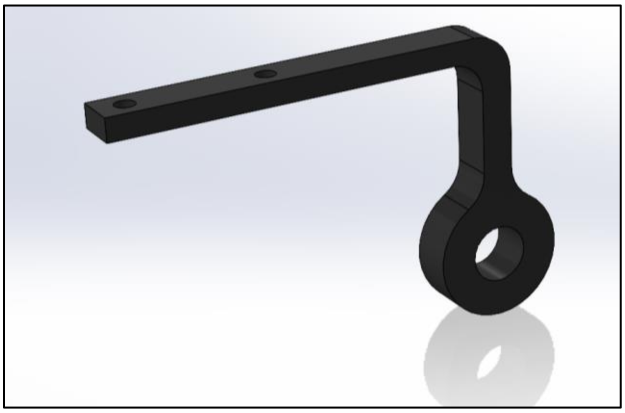

Figure 23 - A 3D model of the attachment arm used to transfer the displacement of the mounting block through to the external magnet of the LVDT.

3.2.1.5. Displacer Calibration

The displacer calibration exercise comprised determining the accuracy of the new displacer system against the Trimos height gauge of known reference, otherwise also known as calibration (not to be mistaken with calibration of the completed automated system). By determining the accuracy of the new displacer to the old known accuracy, it was possible to incorporate the measurement uncertainty caused by this subsystem as a factor in the final system.

Given the known pitch of the ball screw thread and the angular displacement of the stepper motor produced by one pulse, it was possible to determine the linear displacement that occurred for one full rotation of the motor and how many pulses were required for the full rotation (see Section 3.2.1.1).

The DRV8825 provided the capability of reducing the stepper motor angular displacement from 1.8° per step, to micro-steps as small as 1/32 intervals, i.e., 0.05625° per step (see Section 3.2.1.1).

The displacer calibration comprised of repeated applications of a fixed number of pulses corresponding to a calculated target displacement, followed by the actual displacement measured using the height gauge. The step was repeated for different driver intervals where the number of pulses to achieve the same target displacement was adjusted accordingly (e.g., doubling the pulse number when changing from 1/16 to 1/32).

1 step = 1.8 °, therefore, for 1 rotation:

$$\frac{360°}{1.8°} = 200 \text{ steps per revolution}$$

By configuring the DRV8825 to 1/16 intervals, 1 revolution becomes:

$$200(16) = 3200 \text{ steps per revolution}$$

The ball screw thread used in this system had a pitch of 4 mm.

Therefore, applying one revolution of the stepper motor (or 3200 steps with the 1/16 micro-step configuration) would produce 4 mm of linear displacement across the linear guide rail.

It followed then, that a 10 mm linear displacement could be calculated proportionally as follows:

$$3200\left(\frac{10}{4}\right) = 8000 \text{ steps}$$

This number of steps was applied to the motor via the controller digital output and was the basis of the displacer subsystem calibration for determining its accuracy with reference to the old system. A predetermined number of pulses were applied to the motor that corresponded to a calculated physical displacement of 10mm. After each increment, the displacement was measured by the Trimos height gauge as the displacer reference. Table 1 provides the results measured over the system 300mm range at 10mm intervals (i.e., 8000 pulse intervals).

Pulse No.	Height Guage [mm]	Pulse No. (continued.)	Height Guage [mm]	Pulse No. (continued.)	Height Guage [mm]
8000	10.01	88000	109.996	168000	210.021
16000	20.004	96000	120.011	176000	220.008
24000	30.012	104000	130.03	184000	230.03
32000	40.028	112000	140.028	192000	240.022
40000	50.014	120000	150.017	200000	250.016
48000	60.005	128000	160.004	208000	260.018
56000	70.015	136000	170.01	216000	270.024
64000	80.025	144000	179.989	224000	280.018
72000	90.024	152000	189.972	232000	290.025
80000	100.005	160000	200.012	240000	300.020

Table 1 – The number of repeated applications of a constant number of pulses. The values are obtained to evaluate for repeatability.

The measurements taken and recorded in Table 1 were used for calculating a linear regression providing the measurement uncertainty factor for the displacer subsystem (see Section 4.3.2).

3.2.2. Voltmeter Subsystem

For the complete automated LVDT calibrator to function successfully, a controller was selected to be used in the system that was capable of receiving and processing voltage data measured from the LVDT being calibrated. Section 3.2.2.1 provides details of the controller used in this system. For the processing of data by the controller to be possible, an analogue-to-digital converter (ADC) is used to convert the LVDT analogue signal to digital signal over a 15-bit range.

3.2.2.1. Controller

When selecting the controller (Figure 24), it was necessary to consider the design requirements of system to be fulfilled. The ESP32-WROOM-32E development board provided more than sufficient I/O pins, interrupt pins – necessary for an Interrupt Service Routine to be later used in the code (see Appendix F for code) – a 5V and 3.3V power supply, compatible with the Arduino Interactive Development Environment (IDE), compatible with the chosen ADC.

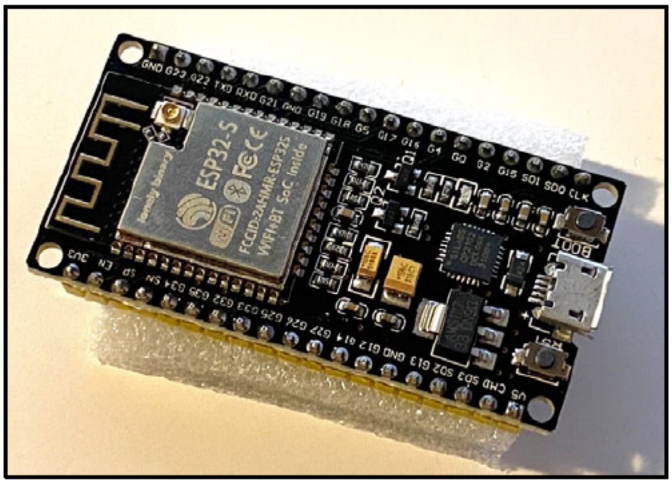

Figure 24 – Image of the ESP32-WROOM-32E development board used as the controller in the new automated LVDT calibration system.

Further justification of choice:

- The ESP32-WROOM-32E proved to be the most compact out of the controllers with the desired features that were available during the design phase of this project.
- The board contains Wi-Fi and Bluetooth compatibility, thus making it possible for future attempts to incorporate wireless connectivity in the design.
- Low-cost.

3.2.2.2. Analogue-to-Digital Converter – ADS1115

The capability to acquire voltage measurements by this system is provided by the use of an ADC. The 16-bit ADS1115 analogue-to-digital converter was utilised (Figure 25) and allows for the acquisition of an analogue signal that is then converted to a digital signal of 15-bits, (i.e., $2^{15} = 32768$ intervals). Note that 1 bit is reserved for signed values so the measurable range is restricted to 15 bits.

The digital signals produced by the ADS were stored and processed by the ESP32 controller (Section 3.2.2.1) as input data for the basis of automatic control capability and voltage measurement for the new calibration system. Configuration of the ADS1115 was done using the 'Adafruit_ADS1X15.h' library (Adafruit Industries 2022) and was integrated into Arduino code written for operation of the automatic calibration system.

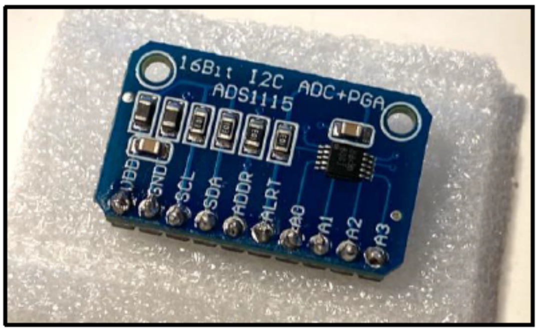

Figure 25 – the 16-bit ADS1115 Analogue-to-Digital converter

Justification of choice:

- Features an input multiplexer that allows for the measurement of either 4 single-ended analogue signals, or two differential analogue signals.
- Incorporated programmable gain amplifier (PGA) which is used to adjust the full-scale range (FSR) of measured input voltages.
- FSR of $\pm$256 mV to $\pm$6.144V.
- Low cost and ease of use.

A differential signal input was used to reject the common mode voltage that could potentially be induced by radiofrequency interference or other types of electromagnetic interference (EMI). The system design incorporating the ADC utilised two analogue inputs for the differential input. Given that the ADS1115 is equipped with 4 analogue inputs, making it possible for an expansion providing a second LVDT signal measurement in tandem.

For the voltmeter to successfully work on the operation of the ADS1115 ADC, it was important to consider the maximum input voltage of the ADS1115, which was approximately 2V. Since the maximum value measured by the LVDT was ~10V, the design of the measuring system had to be such that the LVDT output measured could be done by the ADC without exceeding the ADS1115 maximum input voltage. As per the ADS1115 datasheet (Texas Instruments 2018), the measured analogue input voltage must not exceed the power-supply voltage (VDD) + 0.3V, to prevent permanent damage occurring in the device. Furthermore, the Full-scale Range (FSR), which is the absolute range of measured voltage inputs, needed to be less than VDD for the entire FSR to be measurable. If the FSR exceeded VDD, then the measurable input range would be restricted to VDD (Texas Instruments 2018, p. 17). Given the power input to the ADS1115 was provided by the ESP32 3V3 pin, the ADS1115 was set to 3.3V. Therefore, the FSR selected was the highest PGA within the available range below VDD, which was equal to $\pm$ 2.048V.

Considering the ADS1115 15-bit limitation for positive values, the device provided a bit count of the following range:

$$2^{15} = 32{,}768 \text{ counts}$$

Therefore, with the ADS1115 15-bit capability, the + 2.048V range was mapped over 32,768 counts, which was later worked into the Arduino code loaded onto the ESP32, to determine the which voltage any ADS1115 count would represent.

3.2.2.3. Construction of Voltmeter Prototype

The approach taken was to design a voltage divider of a known ratio between the maximum LVDT voltage output and the ADS1115 FSR of +2.048 V. Using this method, any value measured by the ADC was reflective of the LVDT output by a fixed ratio that was later worked into the code to display the output voltage.

The following steps were taken to achieve this:

$$V_A = \frac{V_{in}}{V_{LVDT}} = \frac{2.048}{10} = 0.2048$$

$$\therefore V_A \approx 1/5$$

The simplest approach was to select 5 E12 resistors of the same value and simply measure across a single resistor. The value would represent a fifth of the total network.

This is represented as follows:

$$V_A = \frac{R}{4R}$$

Where 'R' can be any standard resistor.

The configuration can be seen diagrammatically in Figure 26, where $R = 1.5\ k\Omega$:

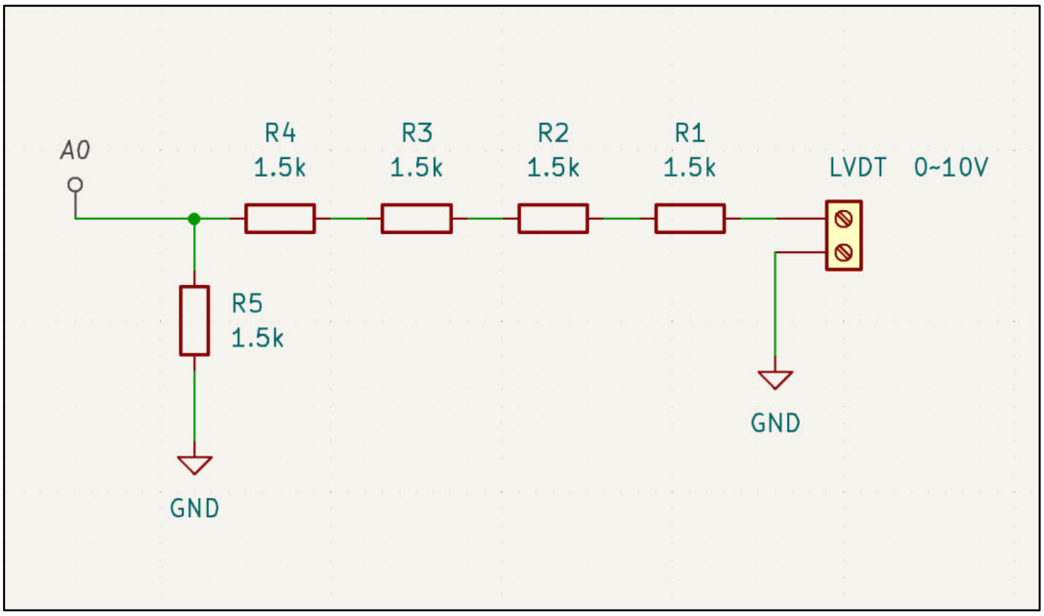

Figure 26 - The voltage divider network used to limit the ADS1115 input voltage to its FSR as a proportion of the LVDT 0~10V signal. 'A0' represents the analogue pin of the ADS1115.

The voltage divider network thus provides a full measurable range of V_{in} that is proportional to V_{LVDT}.

Appendix F contains the code that factors the ratio V_A to display the signal that is being produced by the LVDT.

Figure 27 illustrates the completed construction of a functioning prototype of the voltmeter used in the new LVDT calibration system.

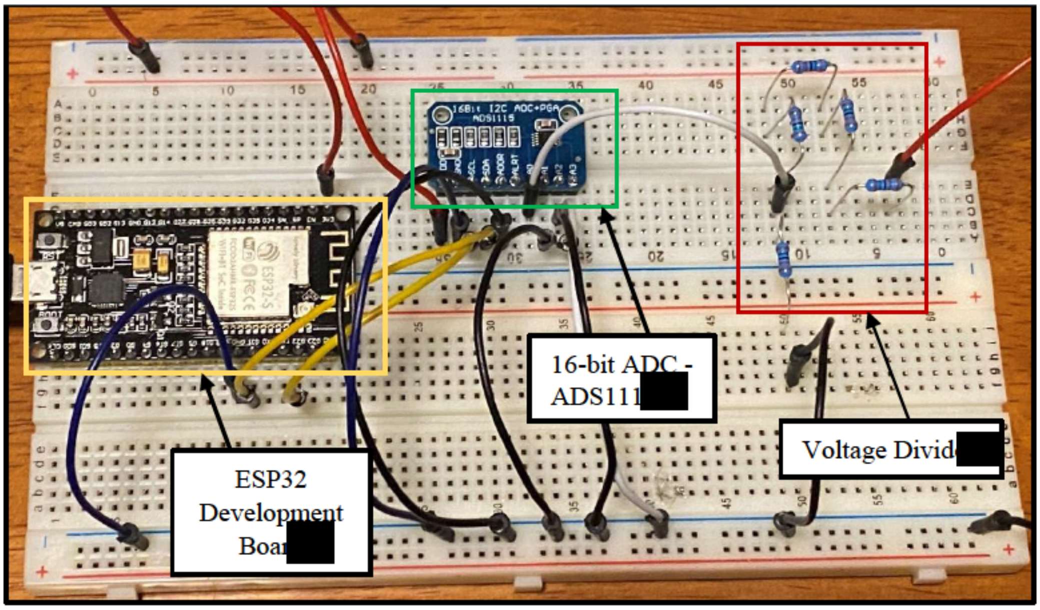

Figure 27 – Functioning prototype of voltmeter utilising the ADS1115, a voltage divider and the ESP32 development board.

3.2.2.4. Voltmeter Calibration

To establish the accuracy of the new voltmeter system using the ADS1115 ADC, voltage measurements had to be obtained and compared to the measurements of the HP voltmeter which was the current standard for voltage measurement in the old manual system (see Section 2.2.1). By understanding these values, it was possible to determine the measurement uncertainty induced in the LVDT calibration process through the use of the ADS1115 ADC.

The calibrated Trimos height gauge was used to perform the displacement of the R-Series LVDT, thereby ensuring variations in the voltages measured between the new and old systems was due to any configuration relating to the voltmeters and not resulting from inconsistence displacement of the LVDT external magnet. After each displacement, the Trimos height gauge was locked, then the voltage signal measured from both the new and old system voltmeters. The LVDT available had a range of 300mm and was measured over this range.

The following table provides the sample measurements of the LVDT signal performed by both the HP 3458A voltmeter and the ADS1115 ADC:

Displacement [mm]	HP 3458A Sample [V]	ADS1115 Sample [V]
0	9.99980	9.99985
60	7.99967	7.99944
120	6.00090	6.00060
180	4.02340	4.02355
240	2.04388	2.04390
300	0.06040	0.06039
240	9.99710	9.99710
180	7.99976	7.99997
120	6.04395	6.04377
60	4.05156	4.05147
0	9.99945	9.99921
60	8.01860	8.01849
120	6.04395	6.04377
180	4.05147	4.05138
240	2.05369	2.05370
300	0.06067	0.06068
240	2.04386	2.04388
180	4.02173	4.02173
120	6.00209	6.00208
60	8.00116	8.00109
0	9.99810	9.99815
60	8.01764	8.01767
120	6.04710	6.04711
180	4.051006	4.05408
240	2.05314	2.05314
300	0.06069	0.06068
240	2.04479	2.04477
180	4.02250	4.02246
120	6.00138	6.00133
60	8.00020	8.00014
0	9.99647	9.99647

Table 2 - The results from measuring the LVDT signal over a 300 mm range using both the ADS1115 and the HP 3458A.

3.2.3. System Circuit

3.2.3.1. Schematic Diagram of Combined Circuit

Figure 28 depicts the complete schematic diagram of the system. The diagram includes all components and respective wiring for the combined fully functioning system.

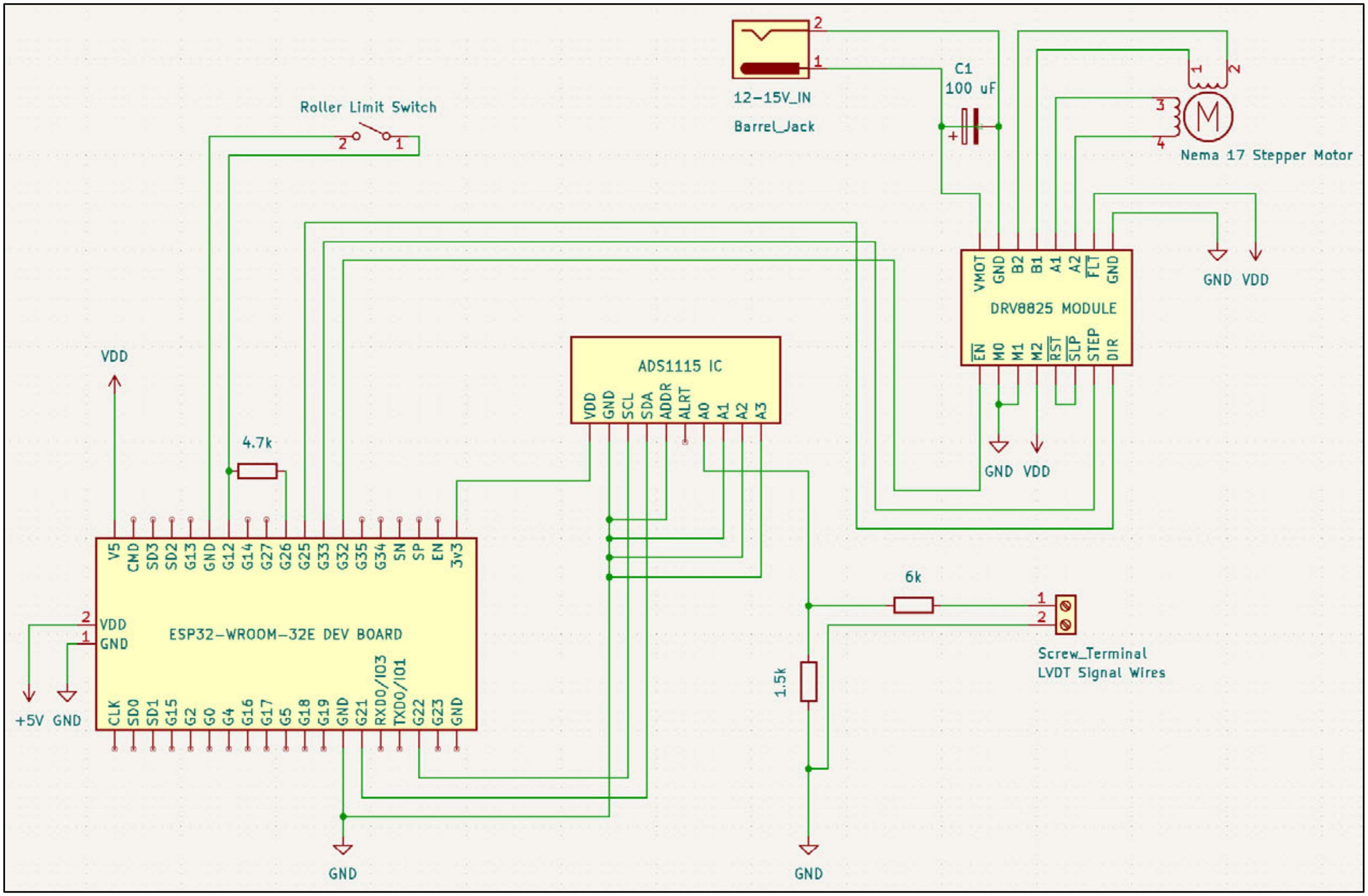

Figure 28 – The schematic diagram of the complete and functioning automated LVDT calibration system.

3.2.3.2. Construction of Combined Voltmeter and Motor Driver Circuit

Figure 29 depicts the working circuit that comprises the 16-bit ADC ADS1115 and the DRV8825 stepper motor driver. Equipped with the ESP32 controller, the linear actuator system operation can be performed via a code, consisting of motor control and measurement of LVDT signal outputs. The code-loaded controller allows for the recording of measurements that can be stored into data files for subsequent processing.

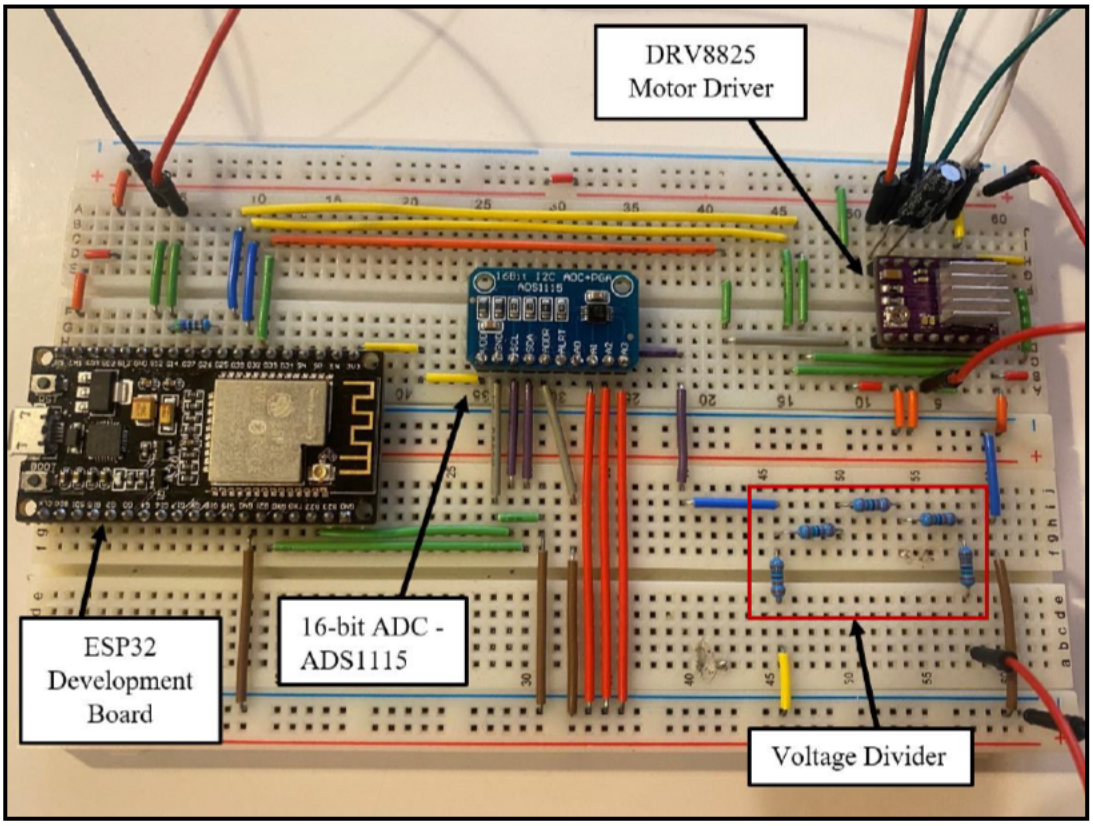

Figure 29 – Breadboard circuit comprising an ADS1115 ADC used as a voltmeter and, a DRV8825 motor driver for stepper motor current control.

3.2.3.3. Circuit Case

In order to provide protection to the automated LVDT circuit and isolate it from the external environment, a case for the circuit was created using the UltiMaker S3 3D printer. The 3D models for the case were created using the SOLIDWORKS 3D CAD software package as (see Figures 30a to 30b). Similarly to the mounting bracket in the linear actuator subsystem, the 3D models of the circuit case were saved as stereolithography files (i.e., '.stl' format) and processed in the Cura software before printing.

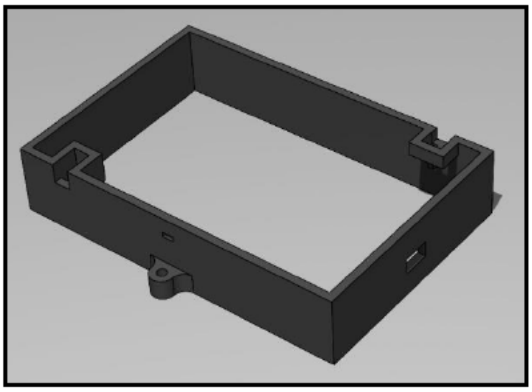

Figure 30a - 3D model of the circuit case.

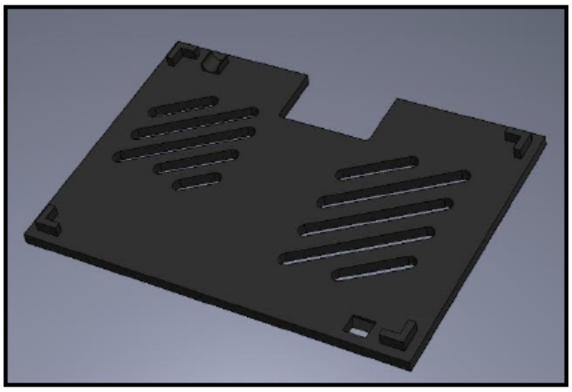

Figure 30b - 3D model of the circuit case cover.

Figure 31 shows the 3D assembly model of the complete circuit case and outlines the locations and purpose of each port. The design of the case has incorporated into it the appropriate geometry to mount a 2-way screw terminal and 2.1 mm female DC port with an interference fit.

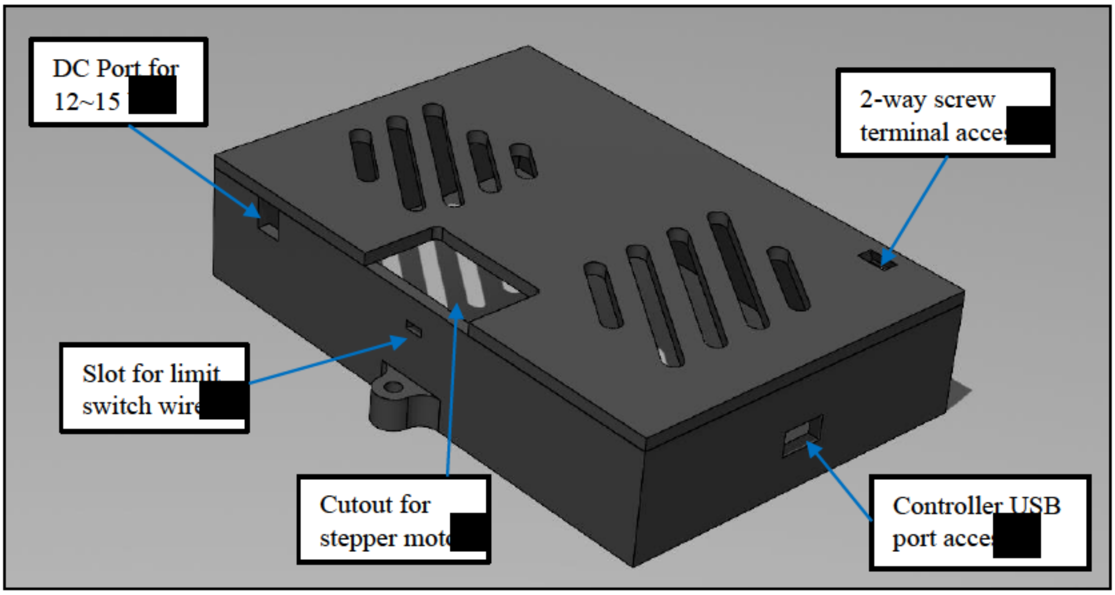

Figure 31 - Annotated 3D assembly model of the LVDT calibration systems circuit case.

3.2.3.4. Completed System

The final step of the construction phase of the system was to correctly mount the circuit case and run the cables to the appropriate locations (see Figure 28) from the screw terminal, DC port and stepper motor, as seen in Figure 32.

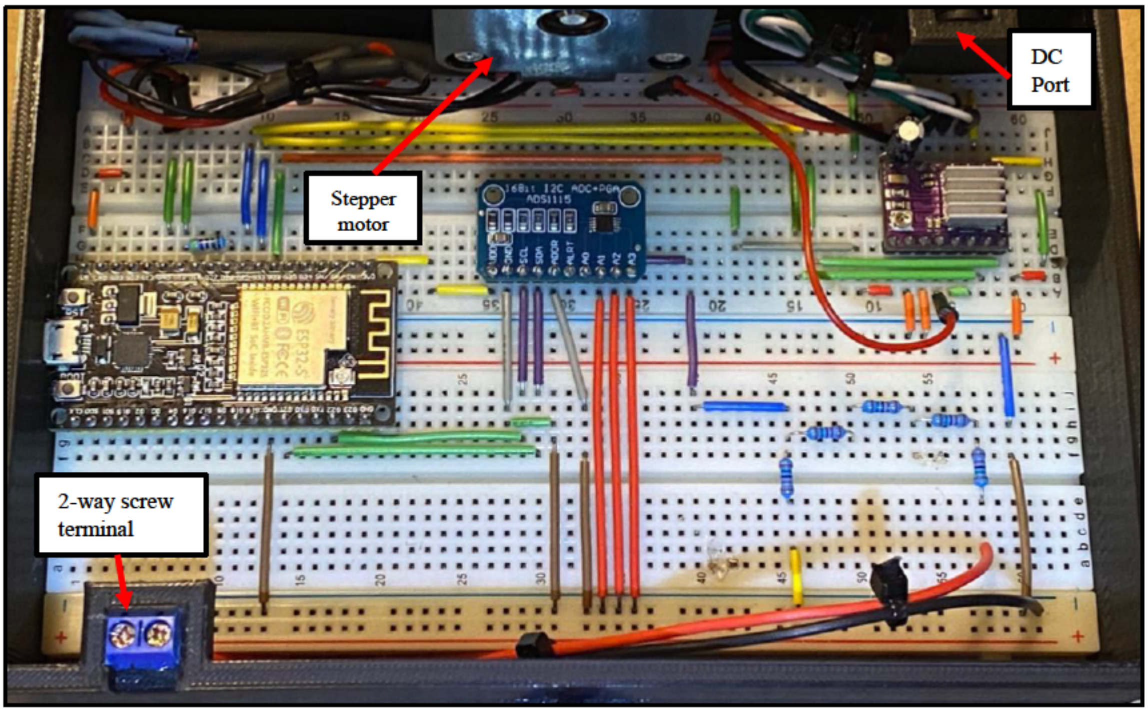

Figure 32 - Completed automated LVDT calibration circuit mounted in the 3D-printed circuit case frame.

The completed automated LVDT calibrator system comprising the displacer subsystem, voltmeter subsystem and remaining circuit for system control can be seen below in Figure 33.

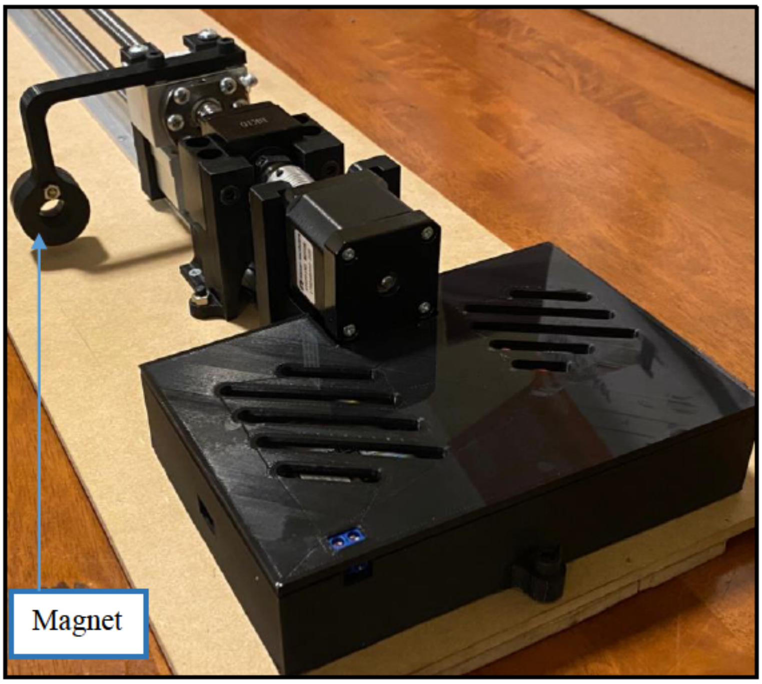

Figure 33 - Image of the fully constructed automated LVDT calibration system with the circuit enclosed in its 3D-printed case.

3.3. Operation of the Automated LVDT Calibrator System

The following series of steps outline the process required for the operation of the automated LVDT calibration system by the user. The first component of the operation will be a manual approach of adjusting the magnet through user input to the controller until the magnet 'origin' is reached, which will be when the signal reads approximately 10000 mV. The code is contained in and run by opening the '.ino' format file. The operation utilises the Arduino IDE, where the user prompt and feedback is done via the 'Serial Monitor', which can be opened by pressing the *shift + ctrl + m* keys. For the Arduino Serial Monitor, it is important during this process, based on the design of the code, that the 'No Line Ending' option is chosen (blue box, Figure 34). This will ensure that each character type entered in the message box (yellow box, Figure 34) as the user input throughout the process is registered accurately without the need for non-visible characters, such as '\n' following the entry. It is also necessary that the correct baud rate of 115200 baud is selected, such that the right channel of communication is used (red box, Figure 34). The section of code and the window selection for the controller (green box, Figure 34) can be ignored as they are only relevant for uploading code, which is already present in the controller.

Figure 34 - Annotated 3D assembly model of the LVDT calibration systems circuit case.

After entering 'begin', the mounting block will perform the homing sequence. The homing sequence consists of the movement of the mounting black towards the motor end of the system until contact is made with the limit switch. Once this occurs, the mounting block travels by a fixed amount away from the limit switch and lands at the 'origin' position (see Figure 35). This step can be seen in Figure 36, where after the homing sequence is finished, the operator is prompted to enter the LVDT operating range (to a limit of 400 mm).

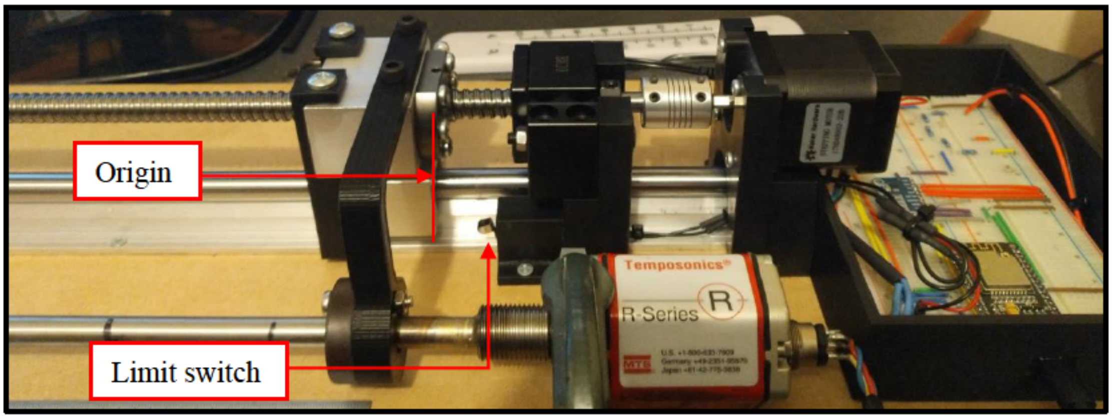

Figure 35 - Annotated image indicating the auto LVDT system homing origin and limit switch position.

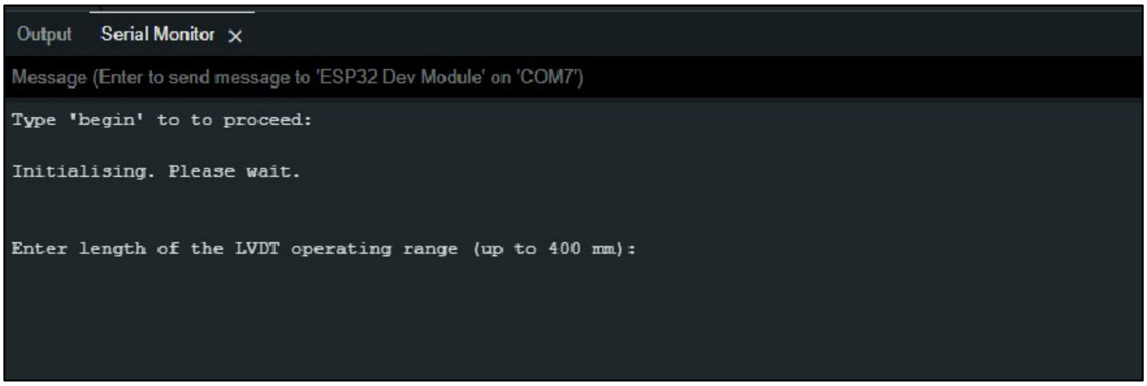

Figure 36 - Annotated 3D assembly model of the LVDT calibration systems circuit case.

Figure 37 illustrates an input of an LVDT range of 300mm, which is the length of the device used in this work (see Section 2.1.1). The operator is then provided with some instructions on adjusting the position of the LVDT external magnet using the serial monitor by selecting the appropriate number on the keyboard and hitting enter. In this step, the direction of travel can be set, as well as a command to read the current signal, or if the LVDT magnet position is already at the signal 10V origin, then the process can be commenced by typing ‘start’ in the serial monitor and hitting enter.

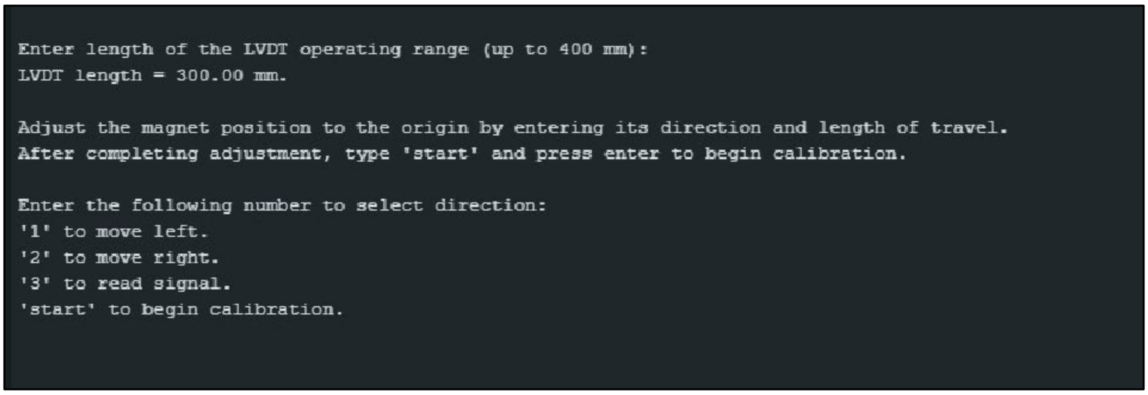

Figure 37 - Auto LVDT system step illustrating the entered operating range and options for selecting direction of magnet travel, reading the current signal or starting the process.

Figure 38 shows the result after having entered ‘3’ to read the current signal (10.01797 mV). It is followed by a repeat of the step shown in Figure 39 and will do so until the operator is satisfied that the magnet is at the origin position (~10.000 V) and chooses to commence the process with ‘start’.

```
Single: Count = 32015, Voltage = 10017.97 mV

Enter the following number to select direction:
'1' to move left.
'2' to move right.
'3' to read signal.
'start' to begin calibration.
```

Figure 38 - Annotated 3D assembly model of the LVDT calibration systems circuit case.

After the position of the magnet has been adjusted due to the length of travel entered by the operator, the value in millimetres will be displayed on serial monitor (as seen in Figure 39 as 2.00 mm followed by 1.00 mm in the opposite direction).

```
Length of adjustment in mm:
2.00 mm

Single: Count = 32002, Voltage = 10013.90 mV

Enter the following number to select direction:
'1' to move left.
'2' to move right.
'3' to read signal.
'start' to begin calibration.

Length of adjustment in mm:
1.00 mm

Single: Count = 31896, Voltage = 9979.48 mV
```

Figure 39 - Annotated 3D assembly model of the LVDT calibration systems circuit case.

Once the value is approximately 10000 mV, the automated process can begin. Figure 40 shows the operation beginning after the position of the magnet produced 9997.94 mV.

```
Single: Count = 31951, Voltage = 9997.94 mV

Enter the following number to select direction:
'1' to move left.
'2' to move right.
'3' to read signal.
'start' to begin calibration.

Operating...
```

Figure 40 - Annotated 3D assembly model of the LVDT calibration systems circuit case.

The next phase of operation is automatically controlled. The LVDT signal will be measured over its full range (as specified by the user as less than or equal to 400 mm) which is based on the position of the external magnet. The magnet travels the full range in one direction measuring 20% intervals, and then measures the same intervals on the return stroke. This is defined as one ‘run’. Three runs are performed automatically in total with each measure being recorded and displayed on the serial monitor, as seen in Figure 41. The values can be simply copied serial monitor and pasted into a text document.

```
Operating...

[Voltage in mV]
7995.67
5991.88
3992.28
1995.04
-0.38
1995.74
3987.44
5991.04
7996.66
9999.04
7994.95
5989.56
3986.25
1988.94
-0.39
1981.87
3987.16
5991.53
7996.80
9999.09
7994.96
5989.70
3986.47
1988.66
-0.31
1980.70
3987.41
5991.43
7997.02
9999.53

Restart operation?

'1' to continue.
'2' to end.


End.
```

Figure 41 - Annotated 3D assembly model of the LVDT calibration systems circuit case.

After the measuring process is complete, the operator is prompted with a selection to repeat another LVDT calibration measurement process, or to conclude the process, by selecting ‘1’ or ‘2’ respectively. If the operator chooses to perform the operation again, the magnet position and the extension arm to which it is attached, will be repositioned at the opposite end of the ball screw/linear rail to allow the user to dismount the LVDT and navigate the rod components out of the magnet. This is prompted with the message “Repositioning. Please wait.” as per Figure 42. The next prompt will instruct the user to enter ‘continue’ in the message box, when the next LVDT is in place.

```
Restart operation?

'1' to continue.
'2' to end.

Repositioning. Please wait.

Enter 'continue' when LVDT is in place:
Repositioning. Please wait.

Enter the following number to select direction:
'1' to move left.
'2' to move right.
'3' to read signal.
'start' to begin calibration.
```

Figure 42 - Annotated 3D assembly model of the LVDT calibration systems circuit case.

4. Results and Discussion

These trials were focused on the 'completion time' and 'user input time' with measurement uncertainty discussed in Section 4.4. In the results obtained for each trial in this experiment, the 'completion time' in the raw data tables represents the total duration of operation. The 'user input time' is the manual user input time required to perform the operation and makes up the whole of the 'completion time' in the manual (old) system operation trials, and only a fraction of the 'completion time' in the automated (new) system operation trials. The trial times were recorded in the following format [mm:ss:ms], along with the three repeated runs recording the LVDT signal at fixed target displacements (as part of the normal calibration process outlined in Section 2.3.1). The signal recording discrepancy between the old and new systems is discussed in section 4.3. Sample results of the old and new system trials can be seen respectively in Tables 3 and 4 in Section 4.1. The full tabulated results for all trials can be found in Appendix A.

4.1. Calibration Trials of Old vs New Automated LVDT System

Appendix A.1. provides the raw data results from trials performed using the old manually operated LVDT calibration system. Important to note is that the entire operation using the old system was a manually driven one by the user, so the 'completion time' and 'user input time' are identical. The values from the three runs are recorded in volts over fixed displacements in millimetres. The trial results for operation times are recorded in the last two rows. Table 5 provides a comparison of the average operation times over all trials for both systems. See Table 3 for a sample of the old system results.

Target Displacement [mm]	Run 1 [V]	Run 2 [V]	Run 3 [V]
0	9.9998	10.0002	10.0002
60	8.0004	8.0012	8.0045
120	5.9991	6.0002	6.0010
180	3.9998	3.9999	4.0001
240	1.9989	1.9995	2.0010
300	0.0046	0.0064	0.0088
240	1.9970	1.9965	1.9991
180	3.9999	3.9998	4.0000
120	5.9998	6.0001	6.0000
60	8.0009	8.0031	8.0040
0	10.0001	10.0007	10.0004
Completion Time = 11:38:45			
User Input Time = 11:38:45			

Table 3 - A sample result showing measurements over three runs when performing the calibration operation with the old system. The completion time and user input time is recorded (data taken for reference only from Table 6 in Appendix A.1.1).

Appendix A.2. provides the results from trials performed using the new automated LVDT calibration system. Note that unlike the old manual system, the new automated system 'completion time' is only made up of a fraction of the 'user input time'. Once the user input was complete, the remaining time of operation was automated and therefore, yielded a consistent additional time of 4 minutes and 35 seconds to completion for each trial. A sample from the new system results can be seen in Table 4.

Target Displacement [mm]	Run 1 [V]	Run 2 [V]	Run 3 [V]
0	9.9998	10.0001	9.9996
60	7.9958	7.9957	7.9958
120	5.9919	5.9918	5.9923
180	3.9926	3.9895	3.9906
240	1.9957	1.9954	1.9956
300	-0.0003	-0.0003	-0.0003
240	1.9873	1.9874	1.9874
180	3.9926	3.9921	3.9920
120	5.9935	5.9937	5.9946
60	7.9971	7.9970	7.9976
0	10.0001	9.9995	9.9998
Completion Time = 06:51:26			
User Input Time = 02:15:56			

Table 4 - A sample result showing measurements over three runs when performing the calibration operation using the new system. The completion time and user input time is recorded (data taken for reference only from Table 14 in Appendix A.2.1).

4.2. Comparison of Results

The following table outlines the average times taken for the operators to complete the LVDT measuring process. The data provides trial times for experienced and inexperienced users to perform the LVDT measurement process using both the old manual system and the new automated system.

	Old System		New System	
	Average Completion Time [mins]	Average User Manual Input Time [mins]	Average Completion Time [mins]	Average User Manual Input Time [mins]
Experienced Operator No.1	11.4517	11.4517	6.3437	1.7521
Experienced Operator No.2	11.0635	11.0635	5.6469	1.0555
Inexperienced Operator No.1	23.0132	23.0132	7.8687	3.2771
Inexperienced Operator No.2	29.4540	29.4540	7.6817	3.0897

Table 5 – The average running times for experienced and inexperienced operators for operation of both the old manual and new automated system.

The column graph in Figure 43 shows the average calibration times for all operators in both the old and new system trials. The old system calibration is a 100% manual process between interval measurements and is therefore represented by full-shaded blue columns. The new system required only an initial manual setup. The times for the manual component are represented by the shaded section in the yellow columns with the remainder representing the automated operation times to completion.

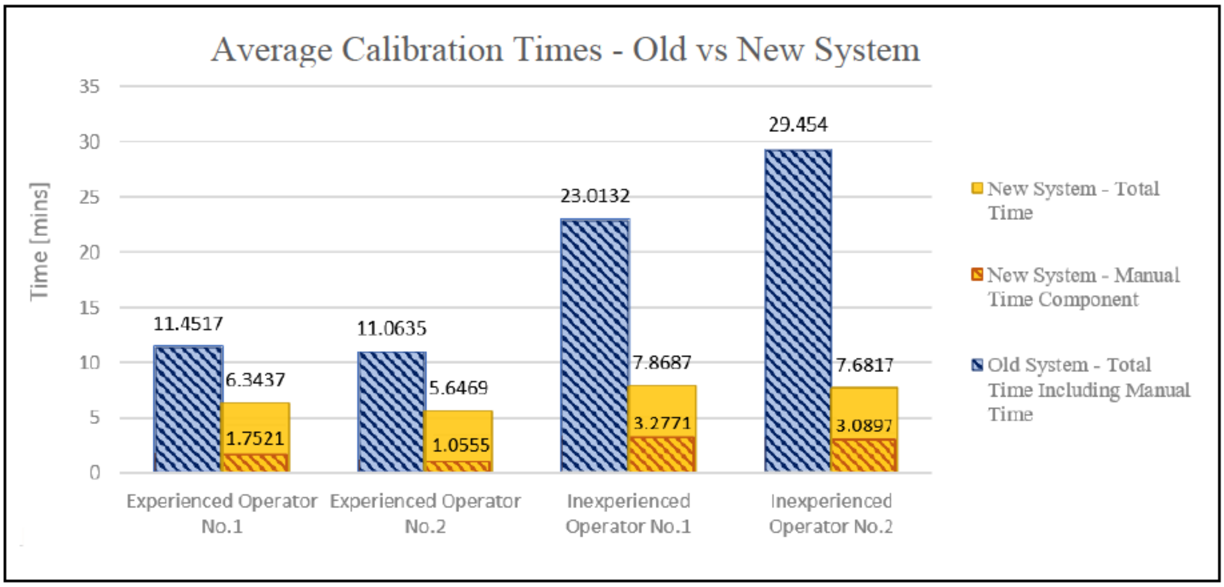

Figure 43 - Annotated 3D assembly model of the LVDT calibration systems circuit

The results in Figure 43 reveal the following key outcomes:

- There was a significant improvement to total operation time when using the new system as opposed to the old system.
- There was significantly less variation in total time of operation between experienced and inexperienced operators, when using the new system as opposed to the old system.
- The only variation in total operation time between experienced and inexperienced operators using the new system, is attributed solely to the initial manual setup (represented by the yellow shaded area in Figure 43). The remainder of the operating time post initial setup was consistent for all operators, as this reflected the automated phase of operation (represented by the unshaded yellow area in Figure 43).

4.3. Measurement Uncertainty

There were various elements within the new system that needed to be considered as a contributing factor to changes in accuracy of the operation. These were: the linear actuator system, driven by the stepper motor; the voltmeter, designed with the ADS1115 ADC. The purpose of measuring these systems against the old system counterparts as a reference standard, was to ascertain the measurement uncertainty introduced by each system.

4.3.1. Displacer Consideration

At least a small variation in measurement seen in Table 1 of Section 3.2.1.5 could likely be attributed to the attachment point between the mounting block and the height gauge arm outlined in Figure 44. It was not possible to ensure there was 100% rigidity in the attachment points. Careful effort was made with the limited tools available to achieve the best possible alignment between the linear displacer and the Trimos height gauge. Despite the efforts to provide rigid attachments and prevent free movement from larger displacements, given the work dealt with displacements at the micrometer level, it should be noted that even the slightest of translation in any of the highlighted attachment points along or about an unintended axis would likely impact the reading at the micrometer level.

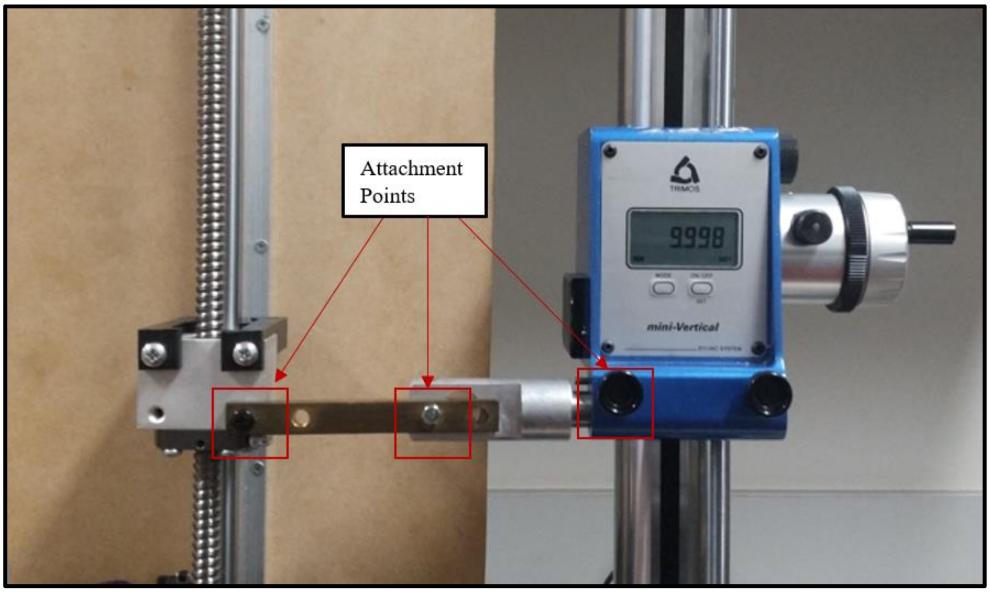

Figure 44 - Annotated attachment points of the arm connecting the Trimos height gauge to the ball screw mounting black

Upon observing the values over 10 mm intervals for the displacer calibration process (see Table 1), it was noted that variations in the results occurred over a range of approximately $\pm 30\ \mu m$. This variation was not accumulative however, meaning that multiple displacements, for example, 10 x 10mm, did not equate to 10 x $\pm 30\ \mu m$ over 100 mm. That is, over the entire 400 mm range tested, a displacement of any magnitude would yield a variation of approximately $\pm 30\ \mu m$.

4.3.2. Subsystem Calibration Factors

When testing the new subsystem functionality, the accuracies of the subsystems were tested with reference to their equivalent in the old system, i.e., the displacer subsystem and voltmeter subsystem. The data taken from the displacer calibration trial (Table 1) and voltmeter calibration trial (Table 2) were used respectively to determine a linear regression for: the number of stepper motor pulses versus the height gauge displacement reading; the ADS1115 voltage reading against the HP 3458A voltage reading. The values were plotted using Excel and a regression calculation performed with the Analysis Toolpak to obtain the Coefficient of Determination (or R^2), which is a measure of the variability of the dependent variable that is explained by the independent variable (Libretexts Statistics 2023).

Figure 45 illustrates the relationship between applied pulses to the stepper motor and the displacement measurement on the Trimos height gauge using the values recorded in Table 1 of Section 3.2.1.5 (see Figure 44 for the setup). The purpose was to evaluate how accurately a precalculated number of stepper motor pulses would result in the expected physical displacement as per the old system Trimos height gauge reference. The results show very small variation between the displacer systems with an R^2 value of 0.99999653. The maximum error from the expected displacement value that occurred, was 30 μm at 104000 pulses.

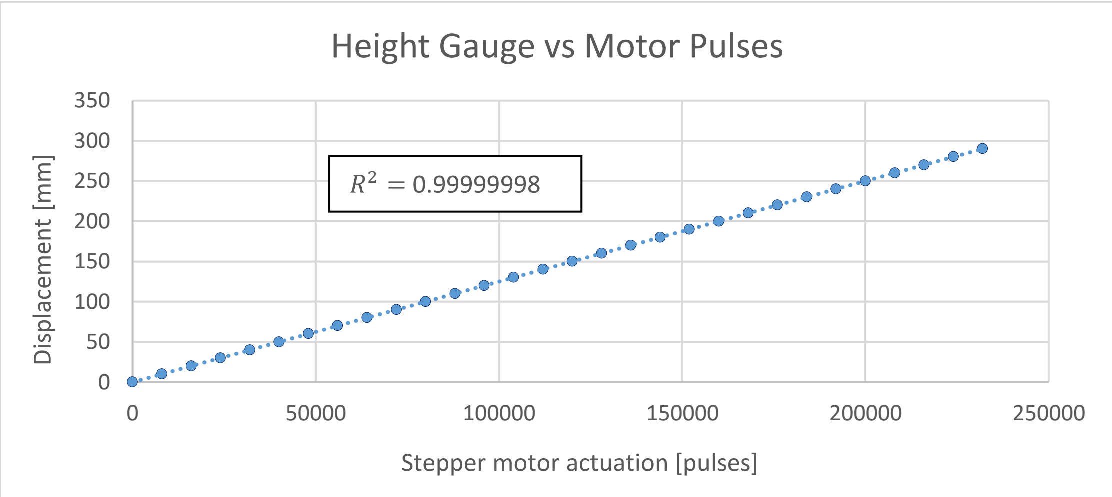

Figure 45 – A plot of the values from Table 1 reflecting the height gauge displacement from the old system with corresponding pulses to the new system stepper motor.

Figure 46 illustrates the voltage measurements for the HP3458A and the ADS1115 at fixed 20% interval displacements across the LVDT 300mm range. The variation between the voltage measurement systems was very low with an R^2 value of 0.99999998. The largest error measured for all points recorded in Table 2 of Section 3.2.2.4, was 300 μV.

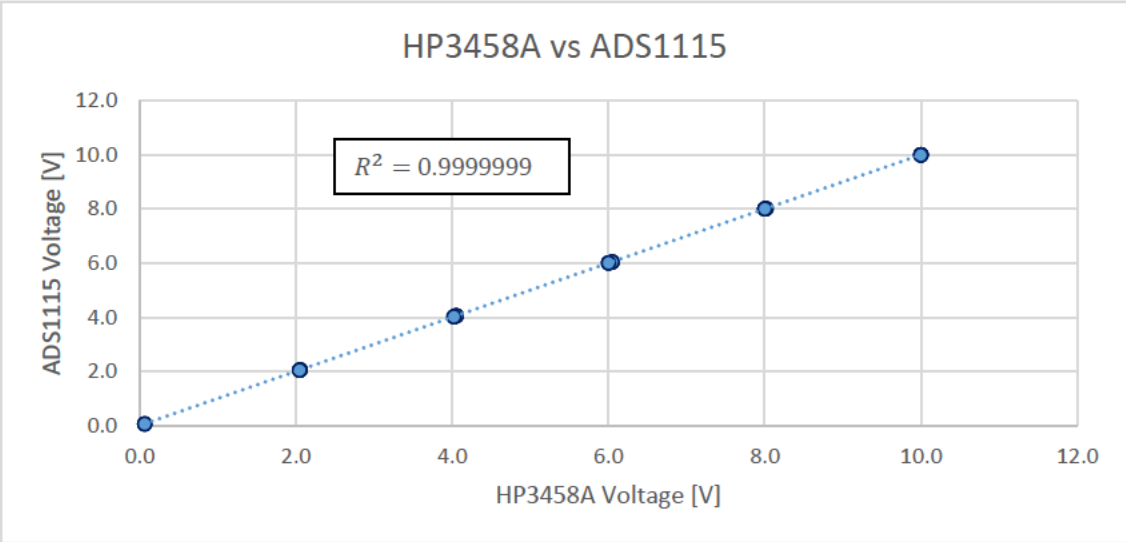

Figure 46 – A plot of the values from Table 2 reflecting the measured voltages at fixed displacements using the voltmeter subsystem of both the new and old calibration systems.

The coefficient of determination values obtained for both subsystems and reflected in Figures 45 and 46, are one of multiple measures subject to a case-by-case approval by NATA for acceptable measurement uncertainty and basis for calibration measurement capability in the scope of accreditation.

4.4. NATA Scope of Accreditation LVDT Calibration Range

One of the considerations in this research was to evaluate the system performance with regards to the FFL's NATA Scope of Accreditation for LVDT calibration. The LVDT calibration and measurement capability is 0.0044 mm over a range of 1 to 600 mm.

The first point to note is that due to component limitation, the system has been designed to accommodate LVDT calibration over a maximum possible range of 0 to 400 mm.

It was also necessary to determine which best-case resolution was possible by considering the ADC 15-bit capability over a 10V range (0-10V being the full range of the LVDT used in this work). This was determined as follows:

$$\frac{10V}{2^{15}} = 0.3052\ mV$$

Therefore, each count will be represented by a minimum interval (or resolution) of 0.3052 mV.

Over a 600 mm range:

$$\frac{600}{2^{15}} = 0.0183\ mm$$

We would therefore have 0.3052 mV change per 0.0183mm, where 0.0183mm is 4.16 times greater than 0.0044 mm.

Given this limitation, we can determine that the reduction in range over which the 10V is measured by the 15-bit ADC to still satisfy the Scope of Accreditation, would be:

$$\frac{x}{2^{15}} = 0.0044$$

$$x = 0.0044(2^{15}) = 144.18$$

Therefore, the 0.0044 mm capability using the 15-bit ADC would be capable at a range of 144 mm or less. This does not have an impact on the capability of the manual system being used, but is a factor to be considered when utilizing the automated system.

As the automated system range limit is 400 mm, the potential LVDT calibration and measurement capability over this range is:

$$\frac{400}{2^{15}} = 0.0122\, mm$$

This will be the interval of displacement for each 0.3052 mV interval measured. The value is ideal, representing resolution and not accuracy, which can further be affected by the maximum error due to the displacer and voltmeter subsystems, as follows:

Displacer maximum variation = $30\ \mu m$

Voltmeter maximum variation = $300\ \mu V$

Displacer maximum error:

$$\frac{300 - 0.00003}{300} \times 100 = 99.99999\%$$

Voltmeter maximum error:

$$\frac{10 - 0.0003}{10} \times 100 = 99.997\%$$

$$0.0122(0.9999999)(0.99997) = 0.01219962 \approx 0.122mm$$

Therefore, when factoring in the maximum error produced by the variation between the new and old subsystems, the proposed measurement capability range of the new automated system is approximately the same and could be deemed negligible.

5. Conclusion

The outcome of the work contained in this report shows the successful design and implementation of a system that provides an automated variation to the LVDT calibration process performed in the DSTG FFL. Operator trial results yielded significant improvements to calibration times and a reduction in operator manual input times, which verifies the system function and satisfies the aim of research. The following points have also been concluded:

- Analysis of the new automated system calibration trials revealed that for every second trial performed by the operator, an improvement occurred in the setup time compared to the time in the first trial. This was true for every operator, despite having had prior LVDT calibration experience or not. By comparison, the second calibration operating time during the old system trials did not show a constant improvement, with one of the inexperienced operators even taking a longer duration to complete the process in the second attempt.

- When utilising the old system for calibration of LVDTs, there was a large variation in operation time between users of different experience levels. Experienced users took only a fracture of the time to complete the calibration compared to inexperienced users, with operation times ranging from approximately a half (11:38:45 versus 22:16:18) to as much as almost a third of the time (11:01:42 versus 31:01:05). The time difference was much less between experienced and inexperienced operators when utilising the new automated system, with the greatest difference in operation time being only 3 minutes and 5 seconds (refer to Tables 17 and 18).

- The new automated system was determined to satisfy ease-of-use expectations, with one inexperienced user unaware of what LVDT calibration was, yet still having been able to successfully perform the calibration operation.

- Unlike the old system, the new system operational time difference between the experienced and inexperienced users, was attributed solely to the time taken by the user to enter the parameters into the prompted command window and to then establish the LVDT operating origin before beginning the automated process. Once the automated process began in each instance of this experiment, the attributed remaining operation time thereafter was identical for every user of the system.

Important to note is the requirement to have any calibration process reassessed by NATA for accreditation where any changes to the process are proposed (as was the case in this work with the development of a new system). Therefore, for FFL issuance of LVDT calibration certificates where the new system would be utilised, changes to the measurement capability of 0.044 mm to 0.122 mm due predominantly to the ADC resolution, must be acknowledged.

By introducing the automated system that provides a high level of consistency in calibration time irrespective of operator experience, and with a significant reduction to manual operator input and overall calibration times, the ramification is a reduction in SMTC downtime in instances where continued testing regimes would be dependent on LVDTs having first been calibrated. Furthermore, the manpower otherwise required with the utilisation of the old system, could then be delegated to other laboratory tasks.

6. Recommended Further Work

In evaluating the process and outcome of this study along with the related system design, the following considerations have been listed for potential further work:

- An upgrade to the code could be made such that the second and third ADS1115 analogue inputs could be utilised to measure a second LVDT of a higher standard. This would allow for the simultaneous measurement and comparison of one LVDT and another of a higher standard and known accuracy for calibration purposes.

- A useful improvement to the system would comprise the modification of the code such that during the setting of the origin phase of the user operation, the system could search and 'hone in' for the 10V origin point. This would alleviate the necessity to manually make small incremental changes about the origin until it is manually found. This modification would further improve operational time, require even less manual input by the user and could be implemented without too much difficulty.

- Achieving an increase to the operating range of the system by replacing the ball screw and linear rail with variations of a longer length. This would require: an adjustment in the code for the new maximum operating range as a condition in the switch statement; subsystem calibration over the new extended range; considering an appropriately sized base onto which longer components would be mounted.

- Improvements to the circuit could be made such as: design for reduction of electromagnetic interference; designing with a PCB to create a more compact circuit.

- An amendment to the code could be included to automatically save the stored files measured during the calibration process. This could be done in Arduino or in another programming language such as Python.

- A wireless interface could be implemented with the user operating system via the ESP-32 equipped Bluetooth or Wi-Fi. This would not limit the user operating device to the length of a USB cable.

- A future iteration of the system could utilise an ADC of a higher resolution with the goal of providing the capability of finer incremental measurements.

Appendix A: Raw Data from System Trials

A.1. Manual (Old) System LVDT Calibration Trials

A.1.1. Trial 1.1 – First Calibration by Experienced Operator No.1

Target Displacement [mm]	Run 1 [V]	Run 2 [V]	Run 3 [V]
0	9.9998	10.0002	10.0002
60	8.0004	8.0012	8.0045
120	5.9991	6.0002	6.0010
180	3.9998	3.9999	4.0001
240	1.9989	1.9995	2.0010
300	0.0046	0.0064	0.0088
240	1.9970	1.9965	1.9991
180	3.9999	3.9998	4.0000
120	5.9998	6.0001	6.0000
60	8.0009	8.0031	8.0040
0	10.0001	10.0007	10.0004
Completion Time = 11:38:45			
User Input Time = 11:38:45			

Table 6 – First old-system calibration results for Experienced Operator No.1.

A.1.2. Trial 1.2 – Second Calibration by Experienced Operator No.1

Target Displacement [mm]	Run 1 [V]	Run 2 [V]	Run 3 [V]
0	10.0001	10.0009	10.0001
60	8.0001	8.0010	8.0021
120	6.0002	6.0002	6.0003
180	4.0001	4.0002	3.9991
240	1.9979	1.9985	1.9989
300	0.0030	0.0064	0.0092
240	1.9978	1.9958	1.9992
180	4.0010	4.0009	4.0015
120	6.0013	6.0009	6.0008
60	7.9991	7.9990	8.0011
0	10.0007	10.0001	10.0002
Completion Time = 11:15:27			
User Input Time = 11:15:27			

Table 7 – Second old-system calibration results for Experienced Operator No.1.

A.1.3. Trial 2.1 – First Calibration by Experienced Operator No.2

Target Displacement [mm]	Run 1 [V]	Run 2 [V]	Run 3 [V]
0	10.0009	10.0007	10.0009
60	8.0011	8.0022	8.0022
120	6.0095	6.0003	6.0002
180	4.0098	3.9990	3.9999
240	2.0099	2.0009	1.9993
300	0.0073	0.0075	0.0063
240	2.0096	2.0001	1.9980
180	4.0001	3.9993	3.9990
120	6.0096	6.0000	6.0000
60	8.0031	8.0025	8.0020
0	10.0006	10.0002	10.0005
Completion Time = 11:05:55			
User Input Time = 11:05:55			

Table 8 – First old-system calibration results for Experienced Operator No.2.

A.1.4. Trial 2.2 – Second Calibration by Experienced Operator No.2

Target Displacement [mm]	Run 1 [V]	Run 2 [V]	Run 3 [V]
0	10.0002	10.0001	10.0005
60	8.0020	7.9989	8.0001
120	5.9991	6.0001	5.9992
180	3.9998	3.9990	3.9990
240	2.0097	2.0088	2.0087
300	0.0052	0.0041	0.0065
240	2.0090	2.0091	1.9999
180	3.9982	3.9989	3.9992
120	5.9996	6.0000	5.9990
60	7.9971	8.0025	7.9982
0	10.0001	10.0005	9.9999
Completion Time = 11:01:42			
User Input Time = 11:01:42			

Table 9 – Second old-system calibration results for Experienced Operator No.2.

A.1.5. Trial 3.1 – First Calibration by Inexperienced Operator No.1

Target Displacement [mm]	Run 1 [V]	Run 2 [V]	Run 3 [V]
0	10.0006	10.0001	9.9999
60	7.9989	7.9991	8.0010
120	5.9998	6.0001	6.0009
180	4.0019	3.9998	4.0007
240	2.0002	2.0015	2.0010
300	0.0042	0.0039	0.0072
240	1.9979	1.9992	1.9985
180	3.9991	3.9995	3.9991
120	6.0005	6.0010	6.0010
60	8.0022	8.0030	8.0039
0	10.0002	9.9998	10.0004
Completion Time = 23:45:17			
User Input Time = 23:45:17			

Table 10 – First old-system calibration results for Inexperienced Operator No.1.

A.1.6. Trial 3.2 – Second Calibration by Inexperienced Operator No.1

Target Displacement [mm]	Run 1 [V]	Run 2 [V]	Run 3 [V]
0	9.9998	10.0002	10.00010
60	7.9992	7.9989	8.0011
120	5.9987	5.9991	6.0001
180	4.0010	4.0002	4.0001
240	2.0013	2.0002	2.0012
300	0.0039	0.0055	0.0043
240	1.9987	1.9982	1.9999
180	3.9990	3.9989	3.9999
120	5.9989	6.0010	5.9939
60	8.0001	8.0022	8.0017
0	10.0001	10.0009	10.0003
Completion Time = 22:16:18			
User Input Time = 22:16:18			

Table 11 – Second old-system calibration results for Inexperienced Operator No.1.

A.1.7. Trial 4.1 – First Calibration by Inexperienced Operator No.2

Target Displacement [mm]	Run 1 [V]	Run 2 [V]	Run 3 [V]
0	10.0001	10.0002	10.0007
60	8.0001	8.0010	8.0015
120	6.0005	6.0012	6.0013
180	4.0012	4.0001	4.0011
240	1.9989	1.9996	1.9976
300	0.0046	0.0059	0.0063
240	2.0002	1.9972	1.9980
180	4.0008	4.0011	4.0013
120	5.9963	6.0009	5.9978
60	7.9990	8.0002	8.0011
0	10.0003	10.0008	10.0001
Completion Time = 28:53:24			
User Input Time = 28:53:24			

Table 12 – First old-system calibration results for Inexperienced Operator No.2.

A.1.8. Trial 4.2 – Second Calibration by Inexperienced Operator No.2

Target Displacement [mm]	Run 1 [V]	Run 2 [V]	Run 3 [V]
0	9.9999	9.9997	10.0006
60	7.9989	7.9992	8.0001
120	6.0021	6.0011	6.0002
180	4.0008	4.0010	4.0009
240	2.0023	2.0017	2.0009
300	0.0038	0.0063	0.0049
240	2.0030	2.0021	2.0019
180	3.9992	3.9999	3.9992
120	5.9996	5.9990	5.9990
60	7.9971	7.9985	7.9982
0	10.0001	9.9999	9.9997
Completion Time = 30:01:05			
User Input Time = 30:01:05			

Table 13 – Second old-system calibration results for Inexperienced Operator No.2.

A.2. Automated System LVDT Calibration Trials

A.2.1. Trial 5.1 – First Auto-Calibration by Experienced Operator No.1

Target Displacement [mm]	Run 1 [V]	Run 2 [V]	Run 3 [V]
0	9.9998	10.0001	9.9996
60	7.9958	7.9957	7.9958
120	5.9919	5.9918	5.9923
180	3.9926	3.9895	3.9906
240	1.9957	1.9954	1.9956
300	-0.0003	-0.0003	-0.0003
240	1.9873	1.9874	1.9874
180	3.9926	3.9921	3.9920
120	5.9935	5.9937	5.9946
60	7.9971	7.9970	7.9976
0	10.0001	9.9995	9.9998
Completion Time = 06:51:26			
User Input Time = 02:15:56			

Table 14 – First new-system calibration results for Experienced Operator No.1.

A.2.2. Trial 5.2 – Second Auto-Calibration by Experienced Operator No.1

Target Displacement [mm]	Run 1 [V]	Run 2 [V]	Run 3 [V]
0	9.9999	10.0003	10.0003
60	7.9989	7.9990	7.9991
120	5.9957	5.9955	5.9996
180	3.9951	3.9954	3.9955
240	1.9980	1.9980	1.9981
300	-0.0003	-0.0003	-0.0003
240	1.9993	1.9990	1.9990
180	3.9974	3.9983	3.9982
120	5.9967	5.9997	5.9997
60	8.0003	8.0003	8.0007
0	10.0003	10.0003	10.0003
Completion Time = 05:49:49			
User Input Time = 01:14:19			

Table 15 – Second new-system calibration results for Experienced Operator No.1.

A.2.3. Trial 6.1 – First Auto-Calibration by Experienced Operator No.2

Target Displacement [mm]	Run 1 [V]	Run 2 [V]	Run 3 [V]
0	9.9999	10.0001	10.0001
60	7.9999	7.9997	7.9998
120	5.9992	5.9993	5.9992
180	3.9989	3.9991	3.9990
240	1.9987	1.9992	1.9991
300	-0.0003	-0.0003	-0.0003
240	1.9997	1.9996	1.9990
180	3.9989	3.9989	3.9991
120	5.9991	5.9992	5.9992
60	7.9985	7.9989	7.9987
0	10.0001	10.0001	9.9999
Completion Time = 05:46:39			
User Input Time = 01:11:09			

Table 16 – First new-system calibration results for Experienced Operator No.2.

A.2.4. Trial 6.2 – Second Auto-Calibration by Experienced Operator No.2

Target Displacement [mm]	Run 1 [V]	Run 2 [V]	Run 3 [V]
0	10.001	10.0004	9.9998
60	7.9996	7.9997	7.9996
120	5.9978	5.9990	5.9993
180	3.9992	3.9992	3.9992
240	1.9971	1.9990	1.9998
300	-0.0003	-0.0003	-0.0004
240	1.9989	1.9991	1.9989
180	3.9992	3.9994	3.9993
120	5.9989	5.9994	5.9994
60	7.9970	7.9981	7.9981
0	10.0004	9.9997	9.9999
Completion Time = 05:30:59			
User Input Time = 00:55:29			

Table 17 – Second new-system calibration results for Experienced Operator No.2.

A.2.5. Trial 7.1 – First Auto-Calibration by Inexperienced Operator No.1

Target Displacement [mm]	Run 1 [V]	Run 2 [V]	Run 3 [V]
0	10.0012	10.0012	10.0012
60	8.0003	7.9990	7.9988
120	5.9988	5.9995	5.9995
180	3.9996	3.9993	3.9993
240	1.9989	1.9987	1.9986
300	-0.0003	-0.0003	-0.0003
240	1.9989	1.9988	1.9988
180	3.9995	3.9994	3.9994
120	5.9997	5.9996	5.9996
60	8.0007	8.0003	8.0000
0	10.0010	10.0013	10.0012
Completion Time = 08:56:13			
User Input Time = 04:20:43			

Table 18 – First new-system calibration results for Inexperienced Operator No.1.

A.2.6. Trial 7.2 – Second Auto-Calibration by Inexperienced Operator No.1

Target Displacement [mm]	Run 1 [V]	Run 2 [V]	Run 3 [V]
0	10.0013	10.0013	10.0013
60	7.9970	7.9976	7.9977
120	5.9994	5.9995	5.9994
180	3.9992	3.9993	3.9993
240	1.9988	1.9988	1.9989
300	-0.0004	-0.0003	-0.0003
240	1.9990	1.9990	1.9990
180	3.9994	3.9995	3.9995
120	5.9996	5.9995	5.9996
60	7.9987	7.9992	7.9995
0	10.0013	10.0014	10.0015
Completion Time = 06:48:02			
User Input Time = 02:12:32			

Table 19 – Second new-system calibration results for Inexperienced Operator No.1.

A.2.7. Trial 8.1 – First Auto-Calibration by Inexperienced Operator No.2

Target Displacement [mm]	Run 1 [V]	Run 2 [V]	Run 3 [V]
0	9.9993	10.0011	10.0009
60	7.9997	7.9979	7.9974
120	5.9994	5.9993	5.9993
180	3.9991	3.9991	39991
240	1.9989	1.9987	1.9988
300	-0.0004	-0.0004	-0.0004
240	1.9999	1.9989	1.9988
180	3.9994	3.9993	3.9994
120	5.9995	5.9995	5.9996
60	7.9993	7.9993	7.9988
0	10.0010	10.0012	10.0012
Completion Time = 08:14:54			
User Input Time = 03:39:22			

Table 20 – First new-system calibration results for Inexperienced Operator No.2.

A.2.8. Trial 8.2 – Second Auto-Calibration by Inexperienced Operator No.2

Target Displacement [mm]	Run 1 [V]	Run 2 [V]	Run 3 [V]
0	10.0010	10.0012	10.0012
60	7.9970	7.9975	7.9972
120	5.9994	5.9994	5.9993
180	3.9992	3.9992	39992
240	1.9988	1.9987	1.9987
300	-0.0004	-0.0004	-0.0004
240	1.9989	1.9989	1.9989
180	3.9993	3.9993	3.9993
120	5.9995	5.9995	5.9996
60	7.9991	7.9992	7.9991
0	10.0017	10.0012	10.0009
Completion Time = 07:06:54			
User Input Time = 02:31:24			

Table 21 – Second new-system calibration results for Inexperienced Operator No.2.

Appendix B: Project Specification

For: Aaron Mietzel

Title: Implementation of Automated LVDT Calibration for Aerospace Testing Laboratory

Major: BENH – Mechatronic

Supervisors: Tobias Low

Enrollment: ENG4111 – EXT S1, 2023

ENG4112 – EXT S2, 2023

Project Aim: To evaluate the feasibility of an automated LVDT calibration system as a replacement to the manual process of calibration currently utilised in Defence Science and Technology Group's structural testing laboratories.

Programme: Version 1, 15th March 2023

Example below

1. Perform initial research on workplace LVDT calibration demands and identify under which parameters the operations are performed. Identify stakeholders and the potential benefits that an improved calibration system would provide.
2. Conduct a literature review on existing LVDT calibration system types and their applications, as well as the technology found in such systems, e.g., software, hardware and expected operator knowledge.
3. Identify system specifications that would be necessary to deliver a calibration result that satisfies industry certification requirements.
4. Identify and compile a list of physical components and software choices that could satisfy the system requirements, then perform a cost and capability analysis followed by an appropriate selection.
5. A system prototype is to be designed and constructed.
6. Initial trials of the prototype are to be conducted to evaluate the feasibility of the system. Should this prove insufficient, variations to the software and hardware can be implemented to achieve an acceptable system performance.
7. Refine the system to successfully complete a calibration.
8. Conduct an experiment using both the old and new system to acquire and evaluate comparative data of the following parameters: calibration time; and accuracy.

If time and resources permit:

1. Publish a work instruction for operator self-training on system operation.
2. Modify the system to provide multiple LVDT calibration simultaneously.

Research Project Budget

Aaron Mietzel - [redacted]

CATEGORY	SOURCE	ESTIMATED	ACTUAL	DIFFERENCE
Analogue-Digital Converter	Self	$20.00	$26.95	-$6.95
500m linear actuator components	Self	$281.16	$117.00	$164.16
Stepper motor	Self	$20.00	$25.00	-$5.00
Microcontroller	Self	$25.00	$18.63	$6.37
3D printer filament	Workplace	$25.00	$34.90	-$9.90
Fasteners	Workplace	$30.00	$25.80	$4.20
Motor driver	Workplace	$15.00	$15.95	-$0.95
Total Expenses		$416.16	$264.23	-

Table 22 – Project specification research budget

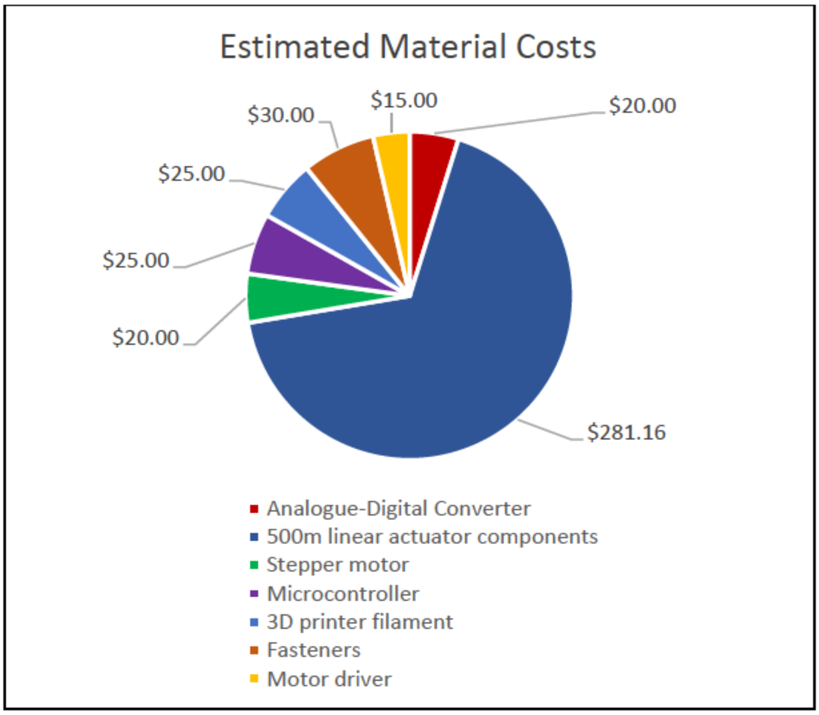

Figure 47 – A pie chart of the project budget item distribution

Access to Resources

Access to the following resources will be required for completion of the research project:

- Computers and software (self)
- Calibration/measuring equipment (self and workplace)
- 3D printer (workplace)
- LVDTs (workplace)

Appendix C: Gantt Chart – Research Project Plan

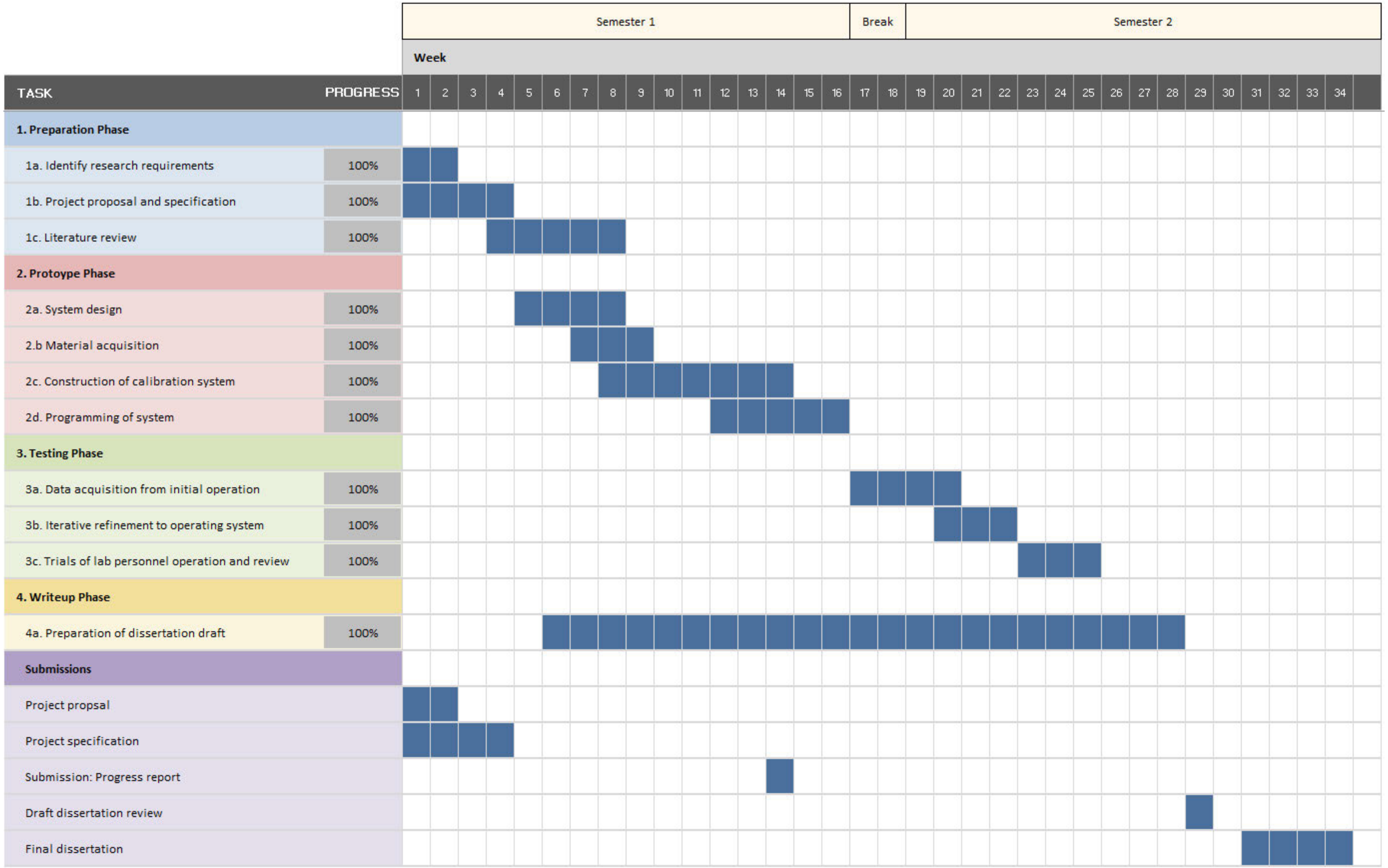

Figure 48 – Gantt Chart outlining the scope of the research project, with percentage completion for each task.

Appendix D: Risk Assessment

Research Project
Aaron Mietzel-[redacted]

Hazard	Likelihood	Severity	Risk Level	Risk Management Activity
Shock hazard: Usage of electrical power; wires/cables; elecronic equipment	3	4	12	Ensure that all electrical equipment to be used has been tested and tagged. Double check the quality of the circuit design to ensure no shorts will occur. Electrical work to be performed by trained personnel.
Crushing hazard: hands in close proximity to moving mechanical components	2	2	4	Operator must keep hands clear of the machine during machine operation. Warning sign may be placed in a visible location to inform other personnel of required safe distance.
Ripping hazard: clothes/hair/loose personal items in close proximity to moving components	2	2	4	It is recommended that operators keep long hair tied back, and loose clothes button or closed. Operators must maintain safe distance from machine during operation to ensure nothing is caught in moving components.
Eye strain	3	1	3	Taking regular breaks to relax eyes when using a computer monitor for extended periods.
Back pain	3	1	3	At 60-minute intervals, stand up and perform a 5-minute stretch. Consider ergonomically adjusted chairs.
Tripping/slipping hazard	3	2	6	Maintain good cable managing practices. Keep cables away from walking area. Ensure floor of laboratory working area is not wet, e.g., water/oil spills.
Falling object hazards	2	1	2	Ensure that any items not being used are not placed nearby or at a high level. Heavy objects (e.g. computer/displacer), should be either fastened, secured or kept away from table/shelf edges.
Spill hazard: food and drink	3	1	4	Food and drinks must not be consumed during operations and should be kept away from the working area to avoid spills causing tripping hazards or damage to equipment.
Fire Hazard	1	5	5	Ensure the working area is equipped with the appropriate fire extinguishers. Monitor all equipment for overheating - observe for burning odours, temperature changes to equipment. Use equipment within well-ventilated areas. Ensure operators are familiar with fire risk control.

Table 23 – Safety Risk Assessment for the research project activities

D.1. Risk Assessment Definition Table

	Severity	Likelihood
1	Minor injury	Very low probability
2	Require brief medical attention	Low probability
3	Injury rendering brief work incapability	Probable
4	Serious injury	High probability
5	Death or permanent disability	Very high probability

Table 24 – Safety Risk Assessment definition table

D.2. Risk Matrix

		LIKELIHOOD				
		1	2	3	4	5
SEVERITY	1	Low	Low	Low	Medium	Medium
	2	Low	Low	Medium	Medium	High
	3	Low	Medium	Medium	Medium	High
	4	Medium	Medium	Medium	High	High
	5	Medium	High	High	High	High

Table 25 – Risk matrix

Appendix E: Fatigue and Fracture Laboratory's NATA Scope of Accreditation

Scope of Accreditation
issued by
National Association of Testing Authorities, Australia

Accreditation Number 233 — Department of Defence, Defence Science and Technology Group

Site Number 226 — **Defence Science and Technology, Aerospace Division: Structures and Materials Test Centre**

Contact Summary

Address		**Phone**	[redacted]
[redacted]		**Mobile**	[redacted]
		Email	[redacted]
		Web	www.dst.defence.gov.au
PORT MELBOURNE		**Contact**	Mr Matthew Pelosi
VIC 3207		**Site Availability**	Services conditionally available to external clients
AUSTRALIA		**Site Supervision**	

Site Scope Last Modified: 25/03/2020

Scope

ISO/IEC 17025
Calibration
The uncertainty of measurement is reported as an expanded uncertainty having a level of confidence of 95% unless stated otherwise

Service	Product	Determination	Technique	Procedure
Dimensional metrology - Engineering equipment and precision instruments	Extensometers	Length measurements	Direct measurement against a reference standard	

Capability

With Calibration and Measurement Capability of -

3 μm from 3 μm to 5 mm

Service	Product	Determination	Technique	Procedure
Dimensional metrology - Engineering equipment and precision instruments	LVDTs	Length measurements	Direct measurement against a reference standard	

Capability

With Calibration and Measurement Capability of-

0.0044 mm from 1 mm to 600 mm

Service	Product	Determination	Technique	Procedure
Force metrology - Force measuring and testing equipment	Load cells	Force in compression; Force in tension	Comparison measurement with reference load cell	

Capability

With Calibration and Measurement Capability of-

0.07% of reading from 0.1 kN to 223 kN in tension and compression

Appendix F: Code for the Automated LVDT Calibration System

```
//created by Aaron Mietzel, 14/08/2023.

#define STEP_PIN          33        //defines pin for applied pulses,
resulting in motor 'steps'.
#define DIR_PIN           25        //defined the stepper motor direction pin
- signal HIGH/LOW affects direction.
#define ENABLE_PIN        32        //defines stepper motor enable pin -
enables motor by setting port to LOW.
#define DIG_SIGNAL        12        //defines pin for limit switch +5V signal.
#define LIMIT             26        //defines input pin for reading limit
switch signal.
#include <Adafruit_ADS1X15.h>       //library for configuration of the ADS1115
ADC.

volatile int limitState;            //declares variable to store state of
limit switch signal. Changed when isr activated.
volatile int phase;                 //declares variable for swtich statement
case.
const int numReadings = 100;        //declares variable for used in measuring
the running average mof the signal.
int16_t measure[numReadings];       //uses the defined 'numReadings' value to
create the size of the array.
int readIndex = 0;
float total = 0;
int full = 0;
float multiplier = 0.062500;        // ADS1115  @ + 2.048V gain (15-bit
results).
float ratio1 = 5.001106;  //multiplies the ratio of 10V by the ADC
differential measure e.g. Vdd/Va0, for voltage divider (both signals measured
with HP for higher standard reference).
float calFactor = 1.001106; //constant adjustment factor of the voltmeter
against the higher standard (i.e., @10 V on HP, HP 10V divided by voltage of
ADC for same signal).
volatile float average;
volatile float voltage;
volatile float voltageAverage;
volatile float choice;
volatile int dummy;           //creates dummy variable for storing Serial.read
value (alleviates an ESP32 error where serial buffer not erasing).
volatile float length;
volatile int flag1;
String prompt;
String msg;
String msg2;            //used in
float distance;         //used in case 1 as parameter for linear travel.
```

```
Adafruit_ADS1115 ads;  //used for the 16-bit version of the ADS11xx

void travel(char DIR, long range, int speedDelay);                 //function
for motor-induced travel, comprising acceleration and constant travel.
void constTravel(char DIR, long range, int speedDelay);            //function
of motor-induced constant travel.
void isrCheck();                                                   //function
for the interrupt service routine.
void RunAverage();                                                 //function
for measuring diff. signal and caluclating running average.
void read();                                                       //function
for measuring diff. signal.


void setup() {

  Serial.begin(115200);
  pinMode(DIR_PIN, OUTPUT);
  pinMode(STEP_PIN, OUTPUT);
  pinMode(ENABLE_PIN, OUTPUT);
  pinMode(DIG_SIGNAL, OUTPUT);
  pinMode(LIMIT, INPUT);
  digitalWrite(DIG_SIGNAL, HIGH);     //provides +5V signal across limit
switch pull-up resistor circuit
  digitalWrite(ENABLE_PIN, LOW);
  ads.setGain(GAIN_TWO);              //2x gain   +/- 2.048V
  attachInterrupt(digitalPinToInterrupt(LIMIT), isrCheck, RISING);
  if (!ads.begin()) {
    Serial.println("Failed to initialize ADS.");
    while (1);
  }
   Serial.println(""); Serial.println("Type 'begin' to to proceed:");
Serial.println("");
}



void loop()
{
  while(prompt!="begin" &&  prompt!="Begin" &&
prompt!="BEGIN"){           //prompts the user to type begin. Used to prevent
automatic starting of system on powerup.
    while(Serial.available()==0){}
//remains in while loop until a value is entered in the message box.
    prompt = Serial.readString();  //stores the value in variable 'prompt'.
    if(prompt!="begin" && prompt!="BEGIN" && prompt!="Begin"){
      Serial.println("Type 'begin' to to proceed:");
Serial.println("");   //if 'begin' was not typed, the user is prompted again.
    }
```

```
    else{
      Serial.println("Initialising. Please wait.");
Serial.println("");    //if 'begin' was typed, the process operation()
function commences.
    }
    dummy = Serial.read();
  }
  operation();              //operation() function performs the main operation
of the system and is structured with via Switch Statement.

}


//
//*********************** FUNCTIONS SECTION
*********************************************

////////////////////////////////// OPERATION
/////////////////////////////////////

void operation(void)
{
  switch(phase)
  {
    case 0:                                    // Homing sequence
      if (limitState == 0)                     //limitState changes to '1' if
ISR is initiated by limited switch.
      {
        digitalWrite(DIR_PIN, HIGH);            // changes motor direction to
move mounting block towards limit switch.
        digitalWrite(STEP_PIN, HIGH);          // applies pulse on and off for
movement. Moving to limit switch sets the origin.
        delayMicroseconds(100);                // the delay between pulses
determines the rotation speed.
        digitalWrite(STEP_PIN, LOW);
        delayMicroseconds(100);                // the delay between pulses
determines the rotation speed.
      }
      else
      {
        travel(0, 7950, 80);                  // travels away from limit switch
by a predefined distance to set the origin.
        limitState = 0;                        // reverts limit switch flag
back to 0 (default).
        while (phase==0){
          Serial.println(""); Serial.println("Enter length of the LVDT
operating range (up to 400 mm):");
          while(Serial.available()==0){
          }
```

```
          length = Serial.parseInt();
          dummy = Serial.read();
          if (length>0 && length<401){
            phase = 1;                                        // phase change to move to
next case
            Serial.print("LVDT length = "); Serial.print(length);
Serial.println(" mm."); Serial.println("");
          }
          else{
            Serial.println("Invalid entry.."); Serial.println("");
            delay(1000);
          }
        }
        delay(2000);
        Serial.println("Adjust the magnet position to the origin by entering
its direction and length of travel.");
        delay(3500);
        Serial.println("After completing adjustment, type 'start' and press
enter to begin calibration."); Serial.println("");
        delay(3000);
      }
      break;


    case 1:                                     //case 1 deals with instructing
the user through the required initial parameters and setup.
      limitState = 0;                           // reverts limit switch flag back
to 0 default.
      Serial.println("Enter the following number to select direction:");
      Serial.println("'1' to move left."); Serial.println("'2' to move
right."); Serial.println("'3' to read signal."); Serial.println("'start' to
begin calibration.");
      while(Serial.available() == 0){
      }
      msg = Serial.readString();
      if(msg=="1" || msg=="2"){                   //if condition is met, the
length of adjustment message will occur
        int x = 0;
        while(x == 0){
          Serial.println(""); Serial.println("Length of adjustment in mm:");
          dummy = Serial.read();                    //reading serial monitor
and storing in 'dummy' (alleviates error with ESP32 where serial not dumping).
          while (Serial.available() == 0){          //remains in while loop
until user inputs value in message box.
          }
          choice = Serial.parseFloat();             //stores operators serial
input into 'choice' variable.
          dummy = Serial.read();
          if(choice>0 && choice<length){
```

```
            x = 1;
            Serial.print(choice); Serial.println(" mm"); Serial.println("");
            distance = choice*800;
            delay(250);
            if (msg == "1"){
              constTravel(0, distance, 100);    //sets direction to up-stroke
if '1' was entered.
              read();
            }
            else{
              constTravel(1, distance, 100);    //sets direction to down-
stroke if '2' was entered.
              read();
            }
            Serial.println("");
          }
          else{
            Serial.println(""); Serial.println("Invalid entry.");
Serial.println(""); //provides error message if entered value is not >0 &
<=400.
            delay(1500);
          }
        }
      }
      else if (msg=="3"){     //if '3' is chosen, the signal will be measured.
        Serial.println("");
        read();               //signal is measured.
        delay(500);
        Serial.println("");
      }
      else if(msg=="start" || msg=="START" || msg=="Start"){    // if a
variation of 'start' is entered, case 2 is entered and auto process begins.
        phase = 2;
      }
      else{               //if '1', '2', '3' or 'start' is not entered, and
error message will appear and case 1 will repeat.
        delay(250);
        Serial.println(""); Serial.println("Invalid entry.");
Serial.println("");
        delay(1500);
      }
      break;

    //case 2 performs the automatic measuring process of the LVDT signal.
    case 2:
      Serial.println(""); Serial.println("Operating..."), Serial.println("");
      delay(500);
      Serial.println("[Voltage in mV]");
```

```
      for (int a=0; a<3; a++){                              //3 iterations
represent the three measuring runs of the LVDT range.
        for (int b=0; b<5; b++){
          float interval = 0.2;                             //sets the travel
interval as 0.2 (20% of 'length').
          travel(0, (length*interval*800)-100, 80);         //800 because 1mm is
equivalent to 8000 motor steps. (-100 accounts for steps occuring in accel.
function).
          RunAverage();
        }
        for (int c=0; c<5; c++){
          float interval = 0.2;                             //sets the travel
interval as 0.2 (20% of 'length').
          travel(1, (length*interval*800)-100, 80);         //800 because 1mm is
equivalent to 8000 motor steps.
          RunAverage();
        }
      }
      phase = 3;                                            //transitions to
case 3.
      delay(2000);
      break;

    //case 3 deals with the end of the operation that asks the user to either
continue or to end the process.
    case 3:
      Serial.println(""); Serial.println("Restart operation?");
      Serial.println(""); Serial.println("'1' to continue.");
      Serial.println("'2' to end.");
      while(Serial.available() == 0){}        //code hangs stays in loop until
a message is passed via serial monitor.
      msg2 = Serial.readString();             //stores user input into 'msg2'.
      dummy = Serial.read();                  //reading serial monitor and
storing in 'dummy' (alleviates error with ESP32 where serial not dumping).
      if(msg2=="1"){
        Serial.println(""); Serial.println("Repositioning. Please wait.");
        Serial.println("");
        constTravel(0, 150*800, 80);          //attachment arm and magnet
travel up-stroke to allow the user to remove the LVDT rod.
        Serial.println("Enter 'continue' when LVDT is in place:");
        dummy = Serial.read();
        int z = 0;
        while(z==0){                         //maintains loop until condition
for 'z' flag is met within the loop.
          while(Serial.available() == 0){}   //maintains loop until a value is
detected in the serial monitor.
          msg2 = Serial.readString();        //stores the user input in to
variable msg2.
```

```
          dummy = Serial.read();
          if(msg2=="continue"){             //if 'continue' is entered, magnet
returns to starting position.
            Serial.println("Repositioning. Please
wait.");  Serial.println("");
            constTravel(1, 150*800, 80);
            phase = 1;                      //case 1 is repeateds.
            z = 1;                          //'z' flag condition is met and
while loop is exited.
          }
          else{
            Serial.println(""); Serial.println("Invalid entry.");         //if
invalid entry occurs, error message appears.
            Serial.println(""); Serial.println("Enter 'continue' when LVDT is
in place:");
          }
        }
      }
      else if(msg2== "2"){                          //if '2' is entered, then
the process code remains in below while loop and the process is finished.
        Serial.println(""); Serial.println("End.");
        travel(0, (length*0.5*800)-100, 80);
        while(1){}
      }
      else{
      }
      break;
    default:
      break;
  }
}

/////////////////////////////////////////////////////////////////////////////
//////////////////
void constTravel(char DIR, long range, int speedDelay)
{
  digitalWrite(ENABLE_PIN, LOW);          // supplies current to stepper
motor.
  if (DIR == 1)                           // sets direction of motor based on
the parameter value entered for 'DIR'.
    digitalWrite(DIR_PIN, HIGH);
  else if (DIR == 0)
    digitalWrite(DIR_PIN, LOW);


  for (long z = 0; z < range; z++)        // sets travel distance and speed
based on values entered for 'range' and 'speed delay'.
  {
    digitalWrite(STEP_PIN, HIGH);
```

```
    delayMicroseconds(speedDelay);
    digitalWrite(STEP_PIN, LOW);
    delayMicroseconds(speedDelay);
    if(limitState == 1){                  // if the limit switch is triggered,
counter 'z' in For Loop is forced to end count, consequently stopping motor
rotation.
      z = range;
      for (int y=0; y<8000; y++){
        digitalWrite(DIR_PIN, LOW);
        digitalWrite(STEP_PIN, HIGH);
        delayMicroseconds(speedDelay);
        digitalWrite(STEP_PIN, LOW);
        delayMicroseconds(speedDelay);
      }
    }
  }

  digitalWrite(ENABLE_PIN, HIGH);            // stops current to stepper
motor  (makes quieter when idle).
}

//////////////////////////////// TRAVEL
//////////////////////////////////////////////////////
//Travel variables as follows: travel('direction', 'range', 'delay for speed')
void travel(char DIR, long range, int speedDelay)      // Dir == 1 for
fordward, 0 for backwards
{
  digitalWrite(ENABLE_PIN, LOW);          // supplies current to stepper
motor.
  if (DIR == 1)                           // sets direction of motor.
    digitalWrite(DIR_PIN, HIGH);
  else if (DIR == 0)
    digitalWrite(DIR_PIN, LOW);
  int delta = 2000;
  for (int y = 0; y < 100; y++)
  {
  digitalWrite(STEP_PIN, HIGH);
  delayMicroseconds(delta);
  digitalWrite(STEP_PIN, LOW);
  delayMicroseconds(delta);
  delta = delta - 20;
  }
  for (long z = 0; z < range; z++)        // sets travel distance and speed.
  {
    digitalWrite(STEP_PIN, HIGH);
    delayMicroseconds(speedDelay);
    digitalWrite(STEP_PIN, LOW);
    delayMicroseconds(speedDelay);
```

```
  }
  digitalWrite(ENABLE_PIN, HIGH);           // stops current to stepper
motor  (makes quieter when idle).
}



///////////////////////////////// VOLTAGE READ AVERAGE
////////////////////////////////////
void RunAverage()
{
  for (int y=0; y<numReadings; y++){
    int16_t test[numReadings];                          //takes the running
average where the no. of readings = value stored in 'numReadings'.
    test[readIndex] = ads.readADC_Differential_0_1();     //stores the ADC
differential value sequentially into each cell in the 'test[]' array.
    total = total + test[readIndex];                    //adds the
previously stored value to the total.
    readIndex = readIndex + 1;                          //increments the
value designated for the array position
    if (readIndex == numReadings)                       //once all cells are
filled, the calculation is performed within the 'if loop' to determine voltage
running average.
    {
      average = total/numReadings;
      voltageAverage = average*multiplier*ratio1*calFactor;
      readIndex = 0;
      total = 0;
      delay(250);
      Serial.println(voltageAverage);                   //prints the voltage
running average.
    }
  }
}

////////////////////////////////// VOLTAGE READ
//////////////////////////////////
void read()
{
  int16_t results;
  float val = ads.readADC_Differential_0_1();     //stores ADC differential
measure into variable 'val'.
  voltage = val*multiplier*ratio1*calFactor;      //calculates value in
voltage using the ADC-measured signal.
  Serial.print("Single: Count = ");
Serial.print(ads.readADC_Differential_0_1()); Serial.print(", Voltage = ");
Serial.print(voltage); Serial.println(" mV");
}
```

```
////////////////////////////////// ISR CHECK
/////////////////////////////////////

void isrCheck()
{
  if(phase != 1){     //the isr check is used to monitor the change in state
caused by contact with the limit switch.
    phase = 0;        //engages a transition to case 0.
  }
  limitState = 1;     //changes value of 'limitState' to 1.
}
```

Appendix G: Datasheets

G.1. Stepper Motor –17HD48002-22B

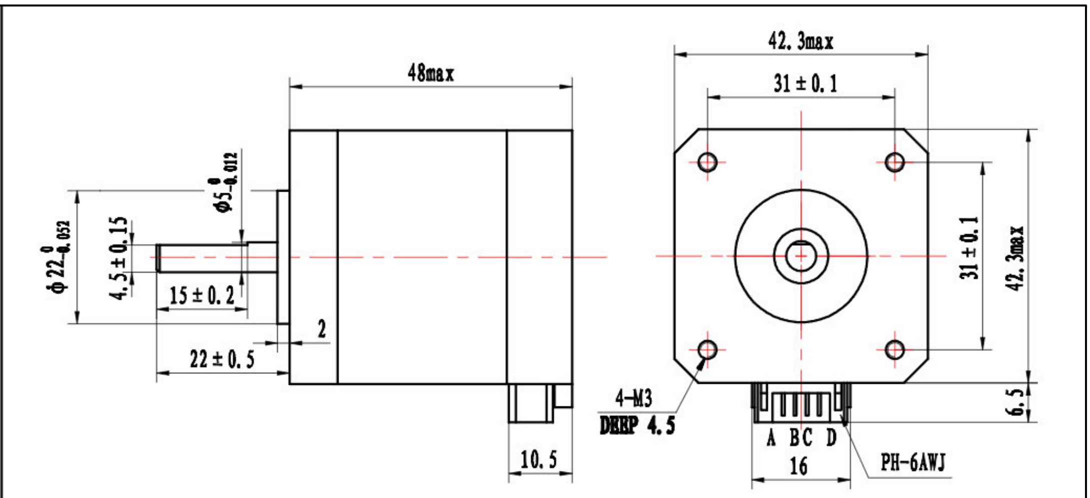

17HD48002-22B

General specification		Electrical specification		Wiring diagram
Step angle	1.8° ±5%	Rated voltage	3.06V	
Number of phase	2	Rated current	1.7A	
Insulation resistane	100MΩmin. (500V DC)	Resistance per phase	1.8Ω ± 10%	
Insulation class	Class B	Inductance per phase	3.8mH ± 20%	
Rotor inertia	82g.cm²	Holding torque	560mN.m	
Mass	0.36kg	Detent torque	24mN.m	

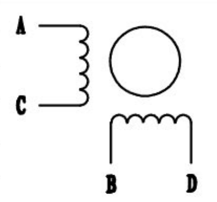

Figure 49 – The datasheet for the 17HD48002-22B stepper motor used as the actuator in the new automated system (Busheng 2021).

G.2. Linear Guide Rail and Sliding Block – SBR12 600mm

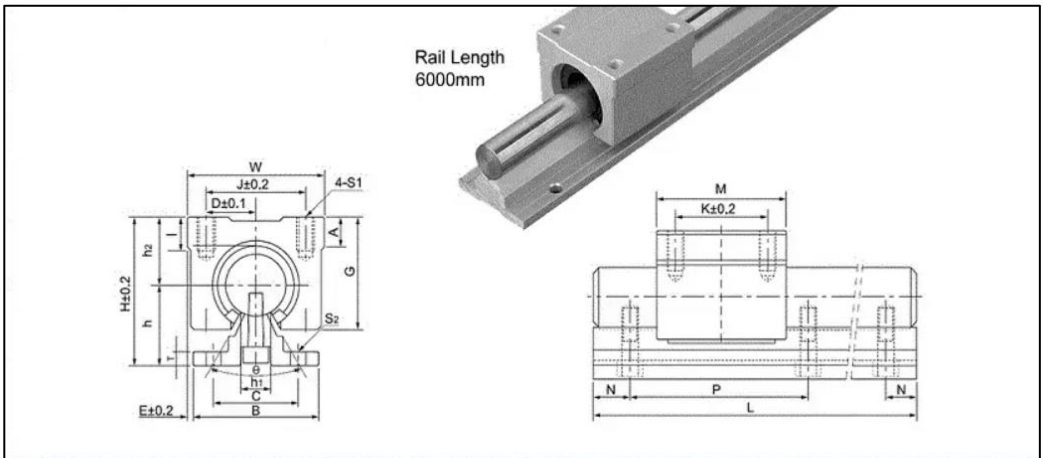

Part No.				Shaft	Load rating		Mass (kg)		Dimension (mm)																	
Rail	NB	Case	Ref NB	d(mm)	C(N)	Co(N)	Case	Rail(kg/m)	D	h	H	E	θ	W	G	A	B	T	M	S1×I	J	K	S2	C	N	P
SBR10S	CE10	SBR10 UU	SME10GUU	Ø10	370	550	0.065	-	18	-	-	-	80°	36	24	7	-		32	M5x10	25	20	-	-	-	-
SBR12S	CE12	SBR12 UU	SME12GUU	Ø12	490	760	0.09	1.59	20	20.46	40	-	80°	40	27.6	8	34	4.5	39	M5x10	28	26	Ø4.5	25	-	100
SBR13S	CE13	SBR13 UU	SME13GUU	Ø13	510	784	0.1		20				80°	40	28	8			39	M5x10	28	26				
SBR16S	CE16	SBR16 UU	SME16GUU	Ø16	770	1170	0.15	2.55	22.5	25	45	2.5	80°	45	33	9	40	5	45	M5×12	32	30	Ø5.5	30	20	150

Figure 50 – A datasheet excerpt 2D drawing with dimensions from the SBR linear guide rail datasheet (SZ Bearing 2018).

G.3. Ball Screw and Nut – SFU1204 550mm

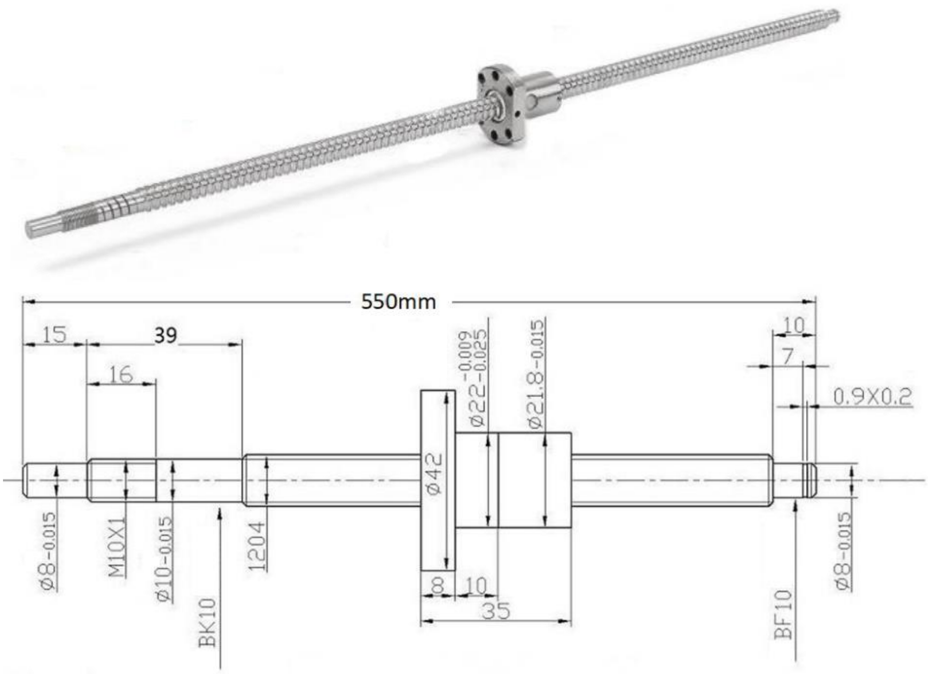

Figure 51 – 2D drawing with dimensions of the SFU1204 550mm ball screw and nut (Handson Technology 2006).

References

Defence Science and Technology Group 2023, *About DSTG*, DSTG, Port Melbourne, Victoria, viewed 26 April 2023, <https://www.dst.defence.gov.au/discover-dst/about-dst>.

Defence Science and Technology Group 2023, *HA Wills Structures and Materials Test Centre*, DSTG, Port Melbourne, Victoria, viewed 26 April 2023, <https://www.dst.defence.gov.au/content/ha-wills-structures-and-materials-test-centre>.

Standards Australia 2018, *General requirements for the competence of testing and calibration laboratories*, AS ISO/IEC 17025:2018, Standards Australia, Sydney, viewed 07 May 2023, <https://infostore.saiglobal.com/en-au/standards/as-iso-iec-17025-2018-99068_SAIG_AS_AS_208312/>.

MTS Systems Corporation 2009, *MTS Series 793 Tuning and Calibration*, pdf version, MTS Systems Corporation, Eden Prairie, Minnesota, viewed 20 May 2023.

NIST/SEMATECH 2012, *e-Handbook of Statistical Methods*, National Institute of Standards and Technology, Gaithersburg, Maryland, viewed 21 May 2023, <https://www.itl.nist.gov/div898/handbook/mpc/section3/mpc3.htm>.

Lord Sensing, *Compact Linear Displacement Sensor*, digital image of an LVDT, Lord Sensing, viewed 20 May 2023, <https://www.microstrain.com/sites/default/files/ls-lvdt-sensor.png>.

Floyd, TL, 2009, *Principles of Electric Circuits: Conventional current version*, Pearson Prentice Hall, Upper Saddle River, New Jersey.

Alciatore, DG & Histand, MB, 2012, *Introduction to Mechatronics and Measurement Systems*, McGraw Hill, New York.

Bolton, W, 1999, *Mechatronics: Electronic Control Systems in mechanical and Electrical Engineering*, Pearson Prentice Hall, Harlow, Essex.

LibreTexts Physics 2022, *14.2: Mutual Inductance*, LibreTexts Physics, California, viewed 02 May 2023, <https://phys.libretexts.org/Bookshelves/University_Physics/Book%3A_University_Physics_(OpenStax)/Book%3A_University_Physics_II_-_Thermodynamics_Electricity_and_Magnetism_(OpenStax)/14%3A_Inductance/14.02%3A_Mutual_Inductance>.

TE Connectivity 2017, *DC-SE SERIES general purpose DC LVDT*, Sensor Solutions DC-SE Series Data Sheet, viewed 05 May 2023, <https://www.te.com/commerce/DocumentDelivery/DDEController?Action=srchrtrv&DocNm=DC_SE_General-purpose-DC-LVDT&DocType=DS&DocLang=English>.

Temposonics 2022, *R-Series Models RP and RH. Analog Outputs (Voltage/Current)*, Data Sheet No. 550992 Revision E, viewed 30 June 2023, <https://www.temposonics.com/docs/temposonicslibraries/literature/r/data_sheet_r-series_rp_rh_analog_550992_en.pdf?sfvrsn=5c7894b0_3>.

Agilent Technologies 2000, *Agilent 3458A Multimeter*, Data Sheet, viewed 30 June 2023, <https://www.metd.com/constructeurs/Hp/hp_3458a%20.pdf>.

Defence Science and Technology Group, Structures and Materials Test Centre 2019, *Calibration of Displacement Transducers*, AD-SMTC-W503, Defence Science and Technology Group, Fishermans Bend, Melbourne.

National Association of Testing Authorities 2023, *What is Accreditation*, NATA, Silver Water, New South Wales, viewed 15 May 2023, <https://nata.com.au/accreditation/>.

National Association of Testing Authorities 2023, *About Us*, NATA, Silver Water, New South Wales, viewed 15 May 2023, <https://nata.com.au/about-us/>.

Texas Instruments 2014, *DRV8825 Stepper Motor Controller IC*, Data Sheet No. SLVSA73F, viewed 12 March 2023, <https://www.ti.com/lit/ds/symlink/drv8825.pdf?ts=1697344596541&ref_url=https%253A%252F%252Fwww.ti.com%252Fproduct%252FDRV8825>.

Texas Instruments 2018, *ADS111x Ultra-Small, Low Power, I^2C-Compatible, 860-SPS, 16-Bit, ADCs With Internal Reference, Oscillator, and Programmable Comparator*, Data Sheet No. SBAS44D, viewed 20 March 2023, <https://www.ti.com/lit/ds/symlink/ads1115.pdf>.

Adafruit Industries 2022, *Adafruit ADS1X15 ADC Driver Library*, ADS1115 Driver Library, viewed 20 March 2023, <https://adafruit.github.io/Adafruit_ADS1X15/html/class_adafruit___a_d_s1115.html>.

LibreTexts Statistics 2023, *10.6: The Coefficient of Determination*, LibreTexts Statistics, California, viewed 07 June 2023, <https://stats.libretexts.org/Bookshelves/Introductory_Statistics/Introductory_Statistics_(Shafer_and_Zhang)/10%3A_Correlation_and_Regression/10.06%3A_The_Coefficient_of_Determination>.

Busheng 2021, *17HD48002-22B Datasheet*, Dongguan Busheng Motor Co. Ltd., stepper motor datasheet, viewed 05 March 2023, <https://pdf1.alldatasheet.com/datasheet-pdf/view/1649034/ETC/17HD48002-22B.html>.

SZ Bearing 2018, *Products*, SZ Bearing Co., Ltd., linear guide rail datasheet, viewed 02 March 2023, <https://www.szdobearing.com/products/linear_rails_and_sliding_block/sbr12_600mm_linear_guide_rails_with_4pcs_sbr12uu_slide_blocks_for_automated_machines_and_equipments_sbr12_600_.html>.

Handson Technology 2006, *SFU1204 Ball Screw Kit*, Handson Technology, ball screw kit datasheet, viewed 04 March 2023, <https://www.handsontec.com/dataspecs/linear%20motion/SFU1204-Ball%20Screw-Kit.pdf>.